BOREAS An international journal of Quaternary research

Interpreting depositional environments from modern floodplain sediments using optically stimulated luminescence

ABIGAIL L. LANGSTON, ABBEY L. MARCOTTE, CHRISTINA M. NEUDORF, KATHLEEN RODRIGUES AND AMANDA KEEN-ZEBERT

BOREAS

Langston, A. L., Marcotte, A. L., Neudorf, C. M., Rodrigues, K. & Keen-Zebert, A. 2025 (January): Interpreting depositional environments from modern floodplain sediments using optically stimulated luminescence. *Boreas*, Vol. 54, pp. 14–33. https://doi.org/10.1111/bor.12679. ISSN 0300-9483.

We investigate how luminescence signals imprinted on fluvial sediments vary depending on the depositional environment and vary through time in the same river. We collected sediment samples from four geomorphically distinct locations on the modern floodplain and modern point bar on the Buffalo River in northwest Arkansas, USA, in order to determine if different depositional environments are associated with distinct bleaching characteristics in the sediments. Our analysis revealed that all samples from different depositional environments yielded ages consistent with modern deposition. The samples collected from the floodplain and bar head contained a higher proportion of grains with residual doses, indicative of incomplete bleaching during transport, while samples from the mid-bar and bar tail appeared well bleached. Our results are particularly intriguing for two significant reasons. First, they highlight distinct equivalent dose distributions in different depositional environments. Second, they shed light on an intriguing relationship: despite generally well-bleached modern floodplain samples, ancient sediments from corresponding terraces displayed equivalent dose (D_e) distributions that suggest partial bleaching in some cases. This research contributes to the growing body of work that seeks to establish a relationship between luminescence properties and sediment transport processes and offers valuable insight into how luminescence signals vary locally in modern fluvial deposits, which can help guide the interpretation of older fluvial deposits.

Abigail L. Langston (alangston@ksu.edu), Department of Geography and Geospatial Sciences, Kansas State University, 920 N. MLK Dr., Manhattan 66506KS, USA; Abbey L. Marcotte, Plant Ecology and Nature Conservation Group, Wageningen University, P.O. Box 47, Wageningen 6700AA, The Netherlands; Christina M. Neudorf, Kathleen Rodrigues and Amanda Keen-Zebert, Division of Earth and Ecosystem Sciences, Desert Research Institute, 2215 Raggio Parkway, Reno 89512NV, USA; *received 7th May 2024, accepted 10th October 2024.*

Luminescence dating is used to determine the time elapsed since minerals (e.g. quartz and feldspar) were last exposed to sunlight or heat, yielding a depositional age for buried sediments. Luminescence dating hinges on the foundational assumption of complete resetting or bleaching of luminescence signals in sediments during transport and deposition. Fluvial sediments are often especially prone to incomplete bleaching during transport, resulting in scatter in equivalent doses that reflects both grains that were fully bleached prior to burial and grains that were not fully bleached prior to deposition and retain a residual signal (Aitken & Smith 1988; Olley *et al.* 1998; Stokes *et al.* 2001; Duller 2008; Gray & Mahan 2015; Gray *et al.* 2019). Determining the source of scatter in equivalent doses (D_e) is not straightforward given that there is not currently a method to empirically identify the sources of D_e scatter in any one sample (Olley *et al.* 1998, 2004; Jain *et al.* 2004; Arnold & Roberts 2009; Summa-Nelson & Rittenour 2012). While processes like beta dose heterogeneity (Guérin *et al.* 2015; Jankowski & Jacobs 2018; Smedley *et al.* 2020) and postdepositional mixing (Kristensen *et al.* 2015; Gliganic *et al.* 2016) can result in D_e scatter, partial bleaching prior to deposition is the dominantly cited reason for D_e scatter in fluvial sediments (e.g. Rittenour 2008; Murray *et al.* 2012; Smedley *et al.* 2020).

The degree of bleaching of modern sediment can be used as an analogue for bleaching conditions during deposition of corresponding ancient sediments, reducing uncertainty about the origins of scatter in D_e distributions (Murray 1996; Olley *et al.* 1998; Porat *et al.* 2001; Stokes *et al.* 2001; Jain *et al.* 2004). Luminescence properties of modern sediments (e.g. degree of bleaching, grain sensitivity, proportion of saturated grains) can also provide valuable insights into geomorphic processes at the time of sediment deposition. Interpreting luminescence properties of sediment samples has been used in studying river avulsion events (Chamberlain & Wallinga 2019), identifying shifts from river aggradation to rapid incision (Bonnet *et al.* 2019), and determining the magnitude or frequency of past flood events (King *et al.* 2014a; McGuire & Rhodes 2015b).

In this study, we used single-grain quartz OSL to analyse samples from four distinct depositional environments across a modern floodplain on the Buffalo River, in northwest Arkansas, USA. Our primary objective was to explore potential variations in D_e distributions associated with partial bleaching in several depositional environments on the modern floodplain and to contribute to the growing body of work that links luminescence signals and geomorphic processes. This study underscores that the bleaching characteristics of modern samples can significantly influence the choice of age model for palaeo-deposits. While our samples from the modern point bar generally appeared well bleached (when compared with modern sediments with many

DOI 10.1111/bor.12679

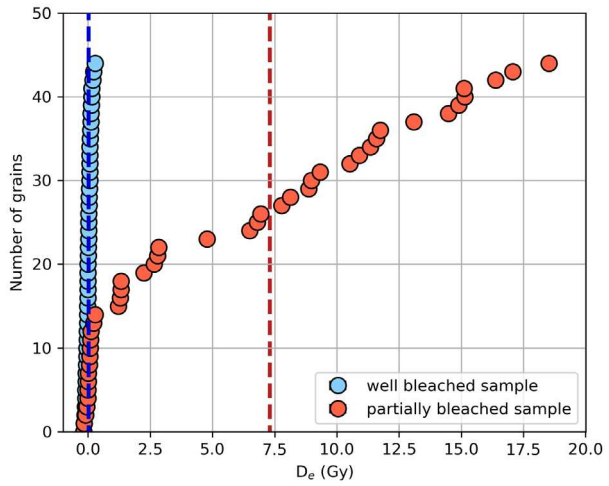

Fig. 1. Idealized equivalent dose (D_e) distributions for modern-aged well-bleached sediments and modern partially bleached sediments. The blue dashed line indicates the true burial dose, 0 Gy, for the well-bleached sample (calculated with CAM and MAM) and partially bleached sample (calculated with MAM). The red dashed line at 7.3 Gy indicates the burial dose calculated with CAM for the partially bleached sample. Equivalent doses in the well-bleached sample cluster tightly around 0 Gy and overdispersion is near 0%. In the partially bleached sample, a population of equivalent doses is clustered around the true burial dose of 0 Gy, but a substantial number of grains were not reset during transport and retain residual doses of up to 20 Gy. Overdispersion is 94%.

grains with high residual doses or saturated grains), ancient sediments from a neighbouring strath terrace had D_e distributions that could suggest partial bleaching. In such a situation, key questions arise that must be addressed in order to select the appropriate model for accurate age calculation. Is partial bleaching indeed present in ancient fluvial samples? Or is the D_e scatter the result of beta dose heterogeneity or postdepositional mixing? To what degree is D_e scatter influenced by unknown contributions of partial bleaching, beta dose heterogeneity, and postdepositional mixing?

Background

Identifying partially bleached sediments

Partial bleaching in a sediment sample can be characterized with a number of different approaches. Partial bleaching can be inferred by examining the distribution of equivalent doses of single grains in a sediment sample (Duller 2004, 2008; Thomsen *et al.* 2007; Murray *et al.* 2021). The log-transformed dose distribution of quartz grains from a well-bleached sample is often expected to exhibit a symmetrical pattern centred around a geometric weighted mean equivalent dose and is characterized by overdispersion values of 20% or lower (Fig. 1; Arnold & Roberts 2009). In contrast, the log-transformed dose distribution of a partially bleached sample shows clear asymmetry and has higher values of overdispersion that often exceed 40–50%, and may surpass 100% (Fig. 1; Arnold & Roberts 2009; King *et al.* 2013; Sim *et al.* 2014). The peak towards smaller equivalent dose values most closely records the true burial dose, while an extended tail of equivalent doses covering a broad range indicates grains that were not fully bleached before deposition and retain a residual dose.

When sediments show substantial scatter in dose distribution, determining the source of the scatter is essential for selecting the most appropriate age model for accurate age determination (Wallinga 2002; Bailey & Arnold 2006; Mayya *et al.* 2006; Arnold & Roberts 2009; Murray *et al.* 2012; Rodrigues *et al.* 2023). The central age model (CAM) assumes that individual equivalent doses in a D_e distribution are log-normally distributed around the geometric weighted mean equivalent dose (Galbraith *et al.* 1999), as would be expected for a well-bleached sample. While CAM is the most common age model used for well-bleached sediments, other age models can also be used for well-bleached sediments. For example, the average dose model (ADM) is used to date well-bleached sediments that have been exposed to heterogeneous dose rates (Guérin *et al.* 2017). ADM uses the arithmetic mean of individual grain D_e values and is therefore sensitive to outliers, both large and small, in the dose distribution. The minimum age model (MAM) is most often used for calculating burial dose in partially bleached samples (Arnold *et al.* 2007), although there are other models for partially bleached deposits, including the leading edge method, the lowest 5% method (Olley *et al.* 1998), and the internal-external consistency criterion (IEU) (Thomsen *et al.* 2007). The MAM assumes that the D_e distribution is from a truncated log-normal distribution, where the lowest D_e values, characterized by the truncated peak, record the most recent bleaching event. Un-logged versions of both CAM and MAM are used for very young or modern sediment samples (Arnold *et al.* 2009).

Partial bleaching in fluvial sediments has been characterized with several metrics beyond dose distribution. The degree of bleaching can be described by the proportion of grains that were well bleached upon deposition (Cunningham *et al.* 2015b) or the percentage of modern grains in a sample (Gliganic *et al.* 2016, 2017). The percentage of saturated grains, grains that cannot absorb additional ionizing radiation, can also be a good metric to characterize the degree of poor bleaching in fluvial sediments (Bonnet *et al.* 2019; Guyez *et al.* 2022). The degree of incomplete bleaching can also be quantified in terms of the residual dose. Samples that were completely bleached before deposition should have a residual dose of less than 5% (Murray *et al.* 2012). Residual doses are calculated as the difference in equivalent doses derived from the central age model and the minimum age model (Chamberlain *et al.* 2018), or for modern fluvial sediments with a depositional age

of 0 years, residual dose is the equivalent dose calculated with CAM (Chamberlain & Wallinga 2019).

Partial bleaching in fluvial environments

Due to the dynamic and stochastic nature of sediment transport in rivers (Gray & Mahan 2015), fluvial sediments are particularly susceptible to incomplete bleaching during transport (Olley *et al.* 1998, 2004; Stokes *et al.* 2001; Wallinga 2002; Jain *et al.* 2004; Duller 2008; Rittenour 2008). Quartz grains are bleached after a few seconds of exposure to sunlight while feldspar bleaching occurs over a few minutes (Godfrey-Smith *et al.* 1988; Smedley *et al.* 2020). Many studies have documented substantial partial bleaching in fluvial sediments, manifested by considerable D_e scatter and elevated residual doses in both quartz sediments (Olley *et al.* 2004; Arnold *et al.* 2007; Summa-Nelson & Rittenour 2012; Sim *et al.* 2014; Larkin *et al.* 2017) and feldspar sediments (Porat *et al.* 2001; McGuire & Rhodes 2015a; Gliganic *et al.* 2017; Guyez *et al.* 2022). The processes that result in partial bleaching can occur before transport, during transport, or even after deposition on the sediment surface (Gray & Mahan 2015). The extent of sunlight exposure for sediments transported and stored in rivers varies from one river system to another and may fluctuate with flow stage within the same river (Cunningham *et al.* 2015a; Gray *et al.* 2017). In larger, continental-scale rivers, sediment primarily undergoes bleaching during the transport phase. The amount of bleaching during transport depends on how far sunlight penetrates the water column, a function of turbidity in the water (Gray & Mahan 2015; Mey *et al.* 2023) and on how far sediment is transported. Conversely, streams with infrequent but intense flood events tend to bleach sediments primarily when sediments are exposed to sunlight after deposition on the riverbed or floodplain (Gray & Mahan 2015; McGuire & Rhodes 2015a). Rapid erosion, transport, and sediment deposition during such flood events, coupled with turbid floodwaters, limit sediment exposure to sunlight, hindering bleaching during transport (Porat *et al.* 2001; Cunningham *et al.* 2015a; Gray & Mahan 2015). In many fluvial systems, sediments undergo bleaching both in transport and after deposition on the surface (McGuire & Rhodes 2015b).

A river carries a mixture of sediments sourced from various locations throughout the watershed, for example soil creep and mass movement from the hillslopes, remobilization of old terrace or floodplain sediments, tributary inputs, or directly from bedrock in the channels (Gray & Mahan 2015; Bonnet *et al.* 2019; Guyez *et al.* 2022). These sediments have followed different paths to the river channel over a range of time scales, resulting in sediments that reach the river channel with different burial histories and degrees of bleaching. Proximity to source materials can further influence the degree of bleaching before deposition; sediment tends to exhibit better bleaching characteristics as it moves downstream away from sediment sources on a scale of 1–100 km (Stokes *et al.* 2001; Hu *et al.* 2010; McGuire & Rhodes 2015b; Gliganic *et al.* 2017; Guyez *et al.* 2023).

Partial bleaching during fluvial transport is the process most commonly used to explain D_e scatter in ancient samples (Rittenour 2008; Murray *et al.* 2012; Smedley *et al.* 2020); however, other processes can also introduce D_e scatter into well-bleached samples. Post-depositional mixing of younger sediments at the top of a profile and older sediments deeper in the profile can introduce significant scatter into D_e distributions (Bateman *et al.* 2003, 2007; Feathers 2003; Reimann *et al.* 2017; Román-Sánchez *et al.* 2019).

Heterogeneity in the beta dose received by sediments over the burial time can also generate D_e scatter. The amount of luminescence signal in sediment grains depends on how long the sediments have been hidden from the sun and accumulating dose via ionizing radiation from the surrounding environment. Ideally the surrounding material is homogeneous and each individual grain in a package of buried sediments accumulates luminescence dose at the same dose rate (Aitken 1985; Guérin *et al.* 2012). However, even if the surrounding material appears homogenous on the centimetre scale, hot spots of higher radiation at the grain scale (microdosimetry) can cause individual sediment grains to accumulate luminescence signal at different rates (Olley *et al.* 1997; Roberts *et al.* 2000; Nathan *et al.* 2003; Thomsen *et al.* 2005; Mayya *et al.* 2006). These localized, millimetre-scale zones of higher than average dose rate are the result of uneven distribution of radioactive elements in the sediment (K, Th, U), especially in environments where the total dose rate is low (Mayya *et al.* 2006; Jacobs *et al.* 2008; Guérin *et al.* 2015). The effects of microdosimetry on a well-bleached sample can result in significant scatter in the dose distribution giving the appearance of a partially bleached sample (Smedley *et al.* 2020). This poses a significant problem for determining accurate depositional ages, as there is currently no way to distinguish between microdosimetry and partial bleaching as the source of scatter in dose distributions (Murray *et al.* 2021).

Modern floodplain sediments as proxy for ancient sediments

Dose distributions of modern floodplain sediments are used to characterize site-specific bleaching conditions and improve interpretation of sources of D_e scatter in analogous ancient sediments (Jain *et al.* 2004; Madsen & Murray 2009; Porat *et al.* 2010; Alexanderson & Murray 2012; Murray *et al.* 2012). If there is substantial scatter in D_e distributions of both modern and ancient sediments, then partial bleaching prior to deposition is

generally assumed to be the cause. However, this approach of using modern sediments as analogues for ancient sediments assumes that sediment bleaching during transport and deposition in the modern environment is the same as when ancient sediments were deposited. Not all modern samples are good analogues for bleaching of older sediments. In some cases, modern samples may give an overestimation of partial bleaching because modern in-channel sediments are likely to be transported and reworked again before final deposition in the sedimentary record (Jain *et al.* 2004; Murray *et al.* 2012, 2021). On the other hand, preserved floodplain and terrace deposits may have been deposited during flood conditions that inhibit sediment bleaching, while modern channel bar sediments may be amply bleached (e.g. Cunningham *et al.* 2015a; Guyez *et al.* 2022).

The numerous studies that document substantial partial bleaching in modern sediments (Porat *et al.* 2001; Olley *et al.* 2004; Arnold *et al.* 2007; Summa-Nelson & Rittenour 2012; Sim *et al.* 2014; Larkin *et al.* 2017; Guyez *et al.* 2022) support the prevailing idea that partial bleaching in fluvial environments is very common and often the primary source of D_e scatter in older sediments. Conversely, other studies have found that modern fluvial sediments exhibit well-bleached characteristics or have residual doses significantly smaller than those accumulated in buried sediments over millennia (Murray 1996; Madsen & Murray 2009; Alexanderson & Murray 2012; Murray *et al.* 2012; Gliganic *et al.* 2017; Arnold *et al.* 2019).

Partial bleaching during transport is often the initial hypothesis to explain D_e scatter in ancient samples (Rittenour 2008; Murray *et al.* 2012; Smedley *et al.* 2020). However, a significant challenge arises when modern sediment samples appear well bleached, yet corresponding ancient sediment samples exhibit D_e scatter consistent with partial bleaching, requiring a reconciliation of the apparent disparities (Jain *et al.* 2004; Duller 2008; Arnold & Roberts 2009).

Dose distribution and geomorphic process

Several studies have shown that luminescence properties of fluvial and glacifluvial sediments (e.g. D_e distributions, residual ages, percent well-bleached grains) can be associated with depositional settings, sediment sources, and transport distances (Stokes *et al.* 2001; Thrasher *et al.* 2009; Summa-Nelson & Rittenour 2012; King *et al.* 2013, 2014a; Cunningham *et al.* 2015a; Bonnet *et al.* 2019; Chamberlain & Wallinga 2019; Guyez *et al.* 2022). For example, in modern-aged glacial outwash sediments, King *et al.* (2014a) found that residual doses and overdispersion in multi-grain quartz samples decreased substantially over ~200 m downstream distance. In another study, Cunningham *et al.* (2015a) found that modern sediments collected from the channel of a bedrock river (Sabie River, South Africa) exhibited nearly perfect bleaching, while recent flood sediments deposited up to 5 m above channel elevation, showed characteristics of poor bleaching. In both examples above, the authors attribute their results to frequent reworking of sediment close to the channel allowing ample opportunity for sediment bleaching during transport. Sediments that were rarely reworked or deposited during flood events were likely transported quickly, possibly in turbid water, allowing for fewer opportunities for bleaching prior to deposition.

Luminescence signals can also be used to interpret fluvial processes during the time of sediment deposition, for example, on the Rangitikei River, New Zealand (Bonnet *et al.* 2019; Guyez *et al.* 2022). Luminescence properties from fluvial terrace sediments (feldspar single grain pIRIR) were interpreted to reflect periods of terrace formation under good bleaching conditions by a braided river, followed by a period of rapid river incision by a single channel stream that hindered effective bleaching of the fluvial sediments (Bonnet *et al.* 2019). The number of saturated sand grains in terrace sediments compared with modern fluvial sediments from the Rangitikei River has been used to identify changing sediment sources through time (Guyez *et al.* 2022) and quantify sediment transport rates (Guyez *et al.* 2023).

These studies collectively illustrate the valuable role of luminescence properties in shedding light on the complex interplay between depositional environments, sediment sources, and transport processes in fluvial systems. Using luminescence properties of fluvial sediments to interpret depositional environment and sediment transport history is an exciting application of luminescence (Gray *et al.* 2019), but establishing clear correlations between luminescence properties and specific geomorphic parameters remains a challenge (King *et al.* 2014a; Cunningham *et al.* 2015b; Gliganic *et al.* 2017; Chamberlain & Wallinga 2019; Brown 2020).

Material and methods

Field location and sample collection

Our field site is located on the Buffalo National River in northwest Arkansas, USA (Fig. 2A). The Buffalo River flows ~240 km from its headwaters to the confluence with the White River, cutting through horizontally layered sedimentary deposits of dolostones, limestones, sandstones and shales that range from Ordovician to Pennsylvanian in age (Fig. S1) (Braden & Ausbrooks 2003). Discharge on the modern Buffalo River is characterized by frequent, rapid changes in streamflow (Li *et al.* 2023) and is prone to flash flooding due to the steep hillslopes, narrow valleys, and karst hydrogeology of the watershed (Neely 1985). At our field site ~100 km downstream of the headwaters, we collected eight sediment samples for single-grain and multi-grain quartz OSL analysis within a 125-m reach of the modern

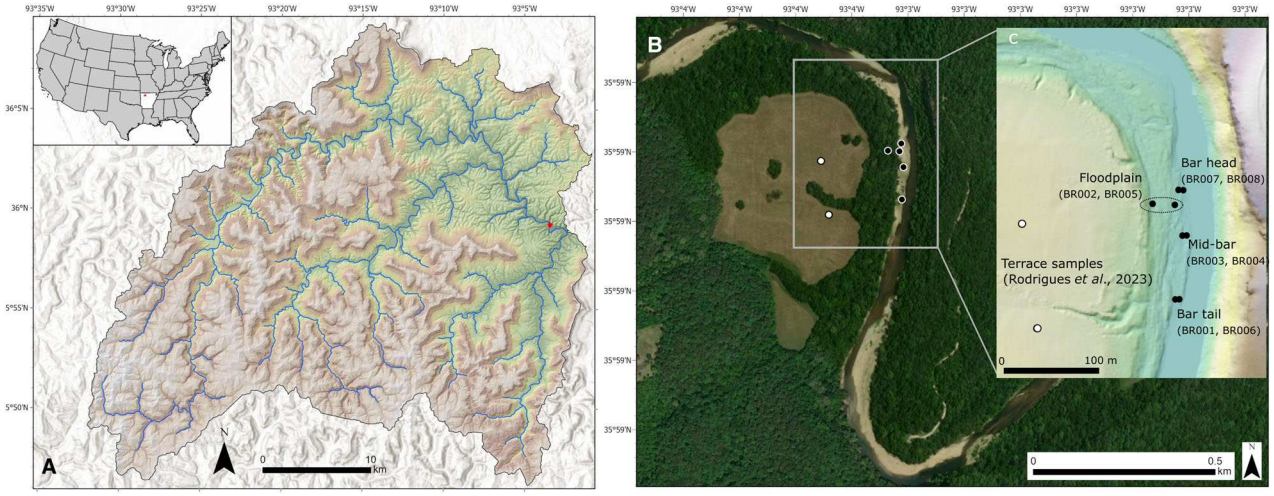

Fig. 2. A. The upper Buffalo River watershed and sampling location in this study. B. Google Earth satellite imagery showing channel and floodplain morphology and locations of sample collection on the Buffalo River, AR and a 1-m DEM of the point bar and modern floodplain showing locations of the samples analysed in this study and the strath terrace sample locations of Rodrigues *et al.* (2023).

floodplain (Fig. 2B). Quartz grains in the sand-sized fraction originate from the Ordovician-aged sandstone beds through which the river is currently incising, as well as Mississippian–Pennsylvanian sandstones that sit high in the watershed, over 400 m in elevation above the modern floodplain elevation (Keen-Zebert *et al.* 2017) (Fig. S1). The eight sediment samples were taken from four distinct depositional environments: floodplain, bar head, mid-bar, and bar tail.

Bar tail. – The bar tail site was situated at the downstream end of a 125-m-long point bar. The bar tail was made up of rippled, medium-grained sand, interspersed with deposits of gravel and coarse sand up to 32 mm in diameter. We collected two samples (BR001, BR006) approximately 2 m apart on the bar tail by hammering sampling tubes (5 cm in diameter, 15 cm in length) vertically into the sediments (Fig. 3A).

Mid-bar. – Approximately 75 m upstream of the bar tail, we collected two sediment samples (BR003, BR004) at a mid-bar location by hammering metal sampling tubes (5 cm in diameter, 15 cm in length) vertically into the sediments (Fig. 3B). These samples were derived from horizontally laminated beds of fine sand, occasionally interspersed with darker organic material and lenses of gravel and coarse sand located between 4 and 25 cm below the surface. Both the bar tail and the mid-bar locations are inundated yearly, and we estimate that these sediments were deposited <1 year prior to sample collection (Fig. S2).

Bar head. – Two samples (BR007, BR008) were collected from the bar head, situated 50 m upstream from the mid-bar samples (Fig. 3C). Given the cobble-armoured nature of the bar head, sediment collection using metal tubes was not possible. Therefore, we collected the samples during the night under red light conditions on a moonless night to prevent any resetting of the luminescence signal caused by daylight exposure (Rajapara *et al.* 2020). The samples were collected by displacing cobbles that ranged in size from 64 to 180 mm in diameter and collecting the sand-sized sediments beneath them. We used a hand shovel to gather the sediment, passed it through a 2-mm sieve, and sealed the sediments in light-proof black bags. Estimations of true depositional ages for the sediments collected under the bar head cobbles are uncertain, but we estimate that the sediments could have been deposited between 1 and 20 years prior to collection (Data S1, Fig. S4).

Floodplain. – We collected two samples (BR002, BR005) from the ~25-m-wide modern floodplain that sits 1.5 m above the channel bar elevation. We estimate that the 1.5 m of floodplain sediment accumulation was completed at least 50 years ago, based on our observations of mature trees on the floodplain surface (Figs 3D, S3). One floodplain sample (BR002) was collected from the near-vertical face that separated the floodplain and the channel bar surface. We cleared several centimetres of collapsed sediment from the 1.5-m-tall vertical step to access undisturbed, horizontally laminated sediments. We collected the sample by driving the metal sampling tube (5 cm in diameter, 15 cm in length) horizontally into the face of the floodplain bank at a depth of 105 cm below the top of the floodplain surface (Fig. 3D). We collected the second floodplain sample (BR005) from the floodplain surface, approximately 20 m from the edge of the floodplain (Fig. 2). This sample was collected from an undisturbed sand dune with an estimated depositional age of less than one year, based on the leaf litter buried under the sand deposits and lack of leaf litter on top

Fig. 3. Sample sites on a modern point bar and floodplain along the Buffalo River. A. Bar tail location with sampling tubes circled. B. Mid-bar location with sampling tubes circled. C. Cobble-armoured bar head location with approximate sampling sites indicated with arrows. D. Floodplain bank location (BR002) with sampling tube circled.

(Fig. S3). We collected the sample by driving a metal sampling tube vertically into the thickest part of the sand dune; no gravel lenses were encountered at this location.

Strath terrace. – Rodrigues *et al.* (2023) collected seven samples from a terrace surface 10 m above the current river channel, located ~200 m from the modern sample collection sites (Fig. 2). Terrace sediments were made up of 2 - 4 m of massively-bedded overbank sands deposited on top of a layer of cobble-sized bedload sediments that sit directly on the bedrock strath. The sampled deposits had no observable stratigraphical structures such as ripples or cross-bedding that would suggest preservation of in-channel sand deposits (Rodrigues *et al.* 2023). However, given that cobble bar deposits are preserved in the terraces, it is likely that in-channel sand bars are also preserved, but not sampled. Here we present dose distributions from two terrace samples for comparison with modern samples. The two terrace samples were collected from a trench dug into the terrace surface at depths of 1.4 m (BUFF026) and 0.8 m (BUFF035) below the terrace surface.

Sample processing

Samples were processed at the Desert Research Institute Luminescence Laboratory in Reno, Nevada, USA, under dim red (>660 nm) illumination to prevent sample light contamination. Approximately 3 cm of sediment at both ends of the metal tube used for sample collection was removed due to potential light contamination. This portion of the sample was reserved for measuring geochemistry for calculating environmental dose rate. The dose rate samples were dried at 80 °C to estimate the water content at the time of collection for environmental dose rate calculations.

The remaining portion of each sample was prepared in the laboratory for single-grain and multi-grain aliquot quartz measurements. Samples were wet sieved to isolate grains within the 180–250 μm diameter range. To

eliminate carbonates, the grains were treated with 10% hydrochloric acid (HCl) for 24 h, followed by a 30% hydrogen peroxide (H_2O_2) treatment for an additional 24 h to remove any remaining organic material. A hand magnet was used to separate heavy minerals from quartz. The remaining non-magnetic fractions underwent a two-step density liquid separation using lithium heteropolytungstates (LST) to separate quartz grains (with densities between $2.62 < \rho < 2.68$ g cm^{-3}) from feldspar grains. To remove the outer alpha-irradiated rim of the quartz grains and any remaining contaminating feldspars after density separation, the quartz grains were etched in 48% hydrofluoric acid (HF) for 60 min. Following the HF treatment, samples were treated with 10% HCl for 3 h to eliminate any precipitated fluorides and then re-sieved within the target fraction.

Measurement of equivalent dose (D_e)

All quartz grain measurements were conducted using two DA-20 Risø TL/OSL readers equipped with green and IR laser single-grain dating attachments, along with a ^{90}Sr/^{90}Y beta source generating dose rates of approximately ~0.13 Gray (Gy) s^{-1} and ~0.11 Gy s^{-1}. The floodplain top sample (BR005) was prepared for multi-grain analysis with 24 aliquots of ~225 grains (4-mm mask). For the multi-grain aliquots, infrared stimulation was conducted with a cluster of infrared (IR) diodes with peak emission at 870 nm and a maximum power of 115 mW cm^{-2} at the sample position. Blue light stimulation was carried out with a cluster of blue LEDs with a peak emission at 470 nm and a total power of 80 mW cm^{-2}. For single-grain OSL measurements, quartz grains were loaded onto gold-plated aluminium discs containing 100 holes, each 300 μm wide and stimulated with a 10-mW stabilized diode-pumped solid state laser emitting at 532 nm. Luminescence signals were detected with a bialkali EMI 9235Q photomultiplier tube (PMT) fitted with Hoya U-340 filters that transmit UV light. D_e values were obtained using a single aliquot regenerative-dose (SAR) protocol that was developed for modern and terrace sediments collected in the Buffalo River watershed (Murray & Wintle 2000; Wintle & Murray 2006; Rodrigues *et al.* 2023) (Table S1).

Post-measurement, all grains underwent screening in Analyst version 4.57 (Duller 2018). For single-grain analysis, we used the initial signal emitted during the first 0.05 s of green laser stimulation time and the subtracted background signal emitted during the last 0.15 s (Fig. 4A). For multi-grain analysis, the initial signal was integrated within the first 1.5 s of stimulation and the background signal was integrated from the last 7 s of stimulation. Grains were accepted based on standard criteria, including: (i) recuperated OSL signal less than 5% of the highest regenerative dose; (ii) maximum test dose error less than 20%; (iii) recycling ratio within the range of 0.8–1.2 (20% of unity); (iv) OSL infrared (IR) stimulation ratio between 0.8 and 1.2. Grains were rejected if they exhibited a poor dose response curve that did not fit well to the data points. The D_e values were plotted based on where the natural signal intersected the dose response curve (Fig. 4B).

The environmental dose rate (D_r) quantifies the rate at which radiation is emitted by radionuclides in the burial environment and cosmic rays from space (Aitken 1982; Durcan *et al.* 2015). The radiation received from alpha and beta particles and gamma rays originates from naturally occurring radioactive elements thorium (Th), uranium (U) and potassium (K) present in and surrounding the sample. To determine the dose rate, the dried portion of each sample obtained from the tube ends was finely pulverized, and approximately 10 g from each sample was sent ALS Geochemistry, Reno, NV, for geochemical analysis of U, Rb, Th and K_2O. Subsamples used for U, Rb and Th measurement were fused with lithium borate and measured by inductively coupled plasma mass spectrometry (ICP-MS). K_2O was measured from the bulk sample with inductively coupled plasma atomic emission spectroscopy (ICP-AES) and converted to %K. The environmental dose rates were computed using DRAC v1.2 (Dose Rate and Age Calculator; Durcan *et al.* 2015), which considers the geochemistry, as well as grain size, water content, altitude, burial depth, and geographical location of the sample. Water content, expressed as a percentage, was assessed by the difference in mass between the wet sample and the sample after drying.

Analysis of dose distributions

The analysis of single-grain results was carried out using the Luminescence package (Kreutzer *et al.* 2023) within the R statistical software environment. To estimate D_e values for the modern floodplain sediments, we used the unlogged central age model (ul-CAM) and the unlogged minimum age model (ul-MAM) (Arnold *et al.* 2009). The D_e distributions for each sample included all sensitive grains capable of holding a luminescence signal, even if the grain had no natural signal. We used the average dose model (ADM, Guérin *et al.* 2017), the central age model (CAM) and minimum age model (MAM) (Galbraith *et al.* 1999) to reanalyse the terrace samples from Rodrigues *et al.* (2023).

To further characterize the dose distributions in each sample, we also considered overdispersion values, number of well-bleached grains, and residual dose. Overdispersion values describe the spread of equivalent doses within the D_e distribution due to extrinsic sources of uncertainty such as partial bleaching, microbeta dosimetry effects, etc. (Galbraith & Roberts 2012). Sample overdispersion was calculated using ul-CAM. We defined well-bleached grains in both the terrace samples and the modern floodplain samples as those with ages matching the D_e calculated from MAM within

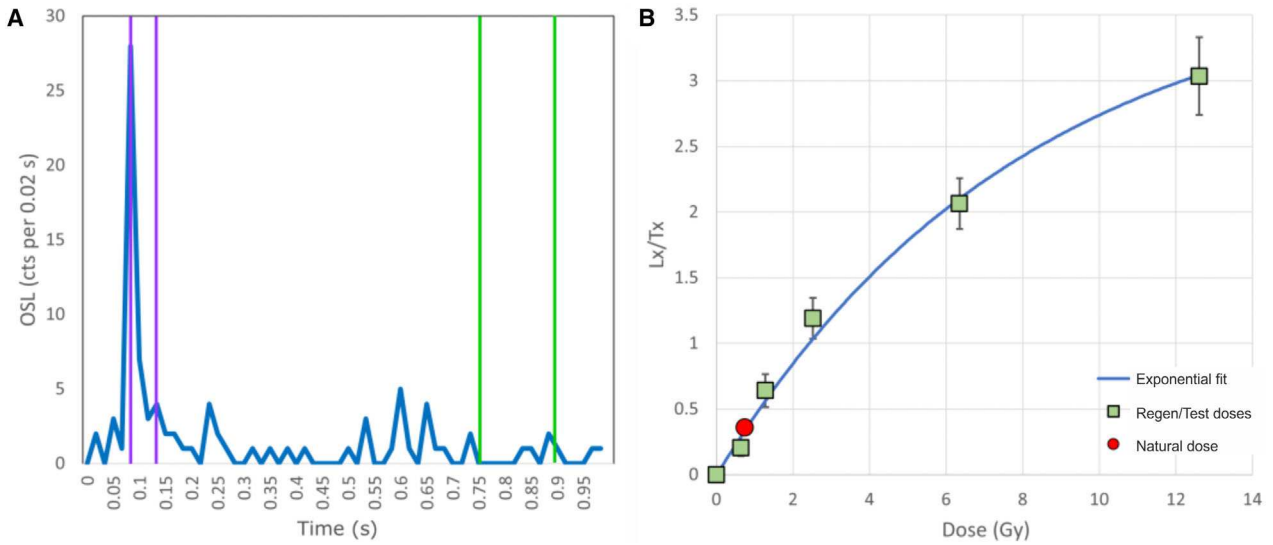

Fig. 4. A. Shine down curve for disc 33, grain 90 from sample BR007. The purple lines indicate the integration limits for the initial OSL signal, and the green lines indicate the limits for the background signal. B. Dose response curve for disc 33, grain 90 from sample BR007. An exponential curve is fit to the Lx/Tx data from the regenerative and test doses, then an equivalent dose (natural dose; 0.75 Gy in this figure) for the grain is estimated from the curve fit.

a 2σ range following Gliganic *et al*. (2016). For the eight modern floodplain samples, the number of well-bleached grains is equivalent to the number of modern grains: grains with a D_e consistent with zero within the reported uncertainties. The residual dose for these samples was calculated as the difference between the D_e derived from ul-CAM and the D_e obtained from ul-MAM (Chamberlain & Wallinga 2019). Most samples yielded a depositional age of zero years, as we would expect for modern floodplain sediments; in these cases the residual dose was estimated based on the CAM age (Chamberlain & Wallinga 2019).

Results

All of our samples yielded minimum doses consistent with zero within 2σ and the majority of accepted grains in all eight samples were well bleached (Table 1). Although the samples predominantly comprised modern grains, we observed differences in their dose distributions and other key metrics related to bleaching. We divided the eight samples into two groups based on their depositional environment: one group of well-bleached samples from the mid-bar and bar tail (BR001, BR003, BR004, BR006), and one group more characteristic of partially bleached samples from the floodplain and bar head (BR002, BR005, BR007, BR008).

Bar tail and mid-bar samples

Samples collected at the mid-bar and bar tail locations appear to have been well bleached before deposition. These samples consist of 91–95% modern grains (Table 1). The dose distributions for each sample in this group exhibit values of D_e tightly centred around 0 Gy representing grains that were fully bleached during transport or immediately following deposition (Fig. 5). Overdispersion in these samples was very low, generally well below 20%, consistent with well-bleached samples (Arnold & Roberts 2009).

Minimum and central values of D_e were calculated using ul-MAM and ul-CAM, respectively. All calculated values of D_e for this sample group were very small, ranging from 0.001±02 to 0.07±0.02 Gy. Unsurprisingly given that four samples were collected from the surface of an active point bar, calculated depositional ages using both CAM and MAM are consistent with 0 years within 2σ uncertainty (Table 1). Residual doses (calculated as the difference between D_e from ul-CAM and D_e from ul-MAM) were also very small and less than zero within 1σ uncertainty. The high percentage of well-bleached grains, low overdispersion values, and residual doses consistent with zero suggest that the samples from the bar tail and mid-bar were well bleached prior to deposition on the modern sandbar.

Bar head and modern floodplain samples

Sediment samples collected from the modern floodplain and the cobble-armoured bar head indicate some degree of incomplete bleaching during transport. These four samples (BR002, BR005, BR007, BR008) were made up of fewer modern grains (79–82%) than the mid-bar and bar tail samples; in the bar head and floodplain samples, 18–21% of individual grains had D_e values inconsistent with a zero-age within 2σ uncertainty (Table 1). These

Table 1. OSL data for the eight modern floodplain samples from the Buffalo River. Sample BR005MG is a multi-grain analysis on sample BR005.

Sample number	Depositional environment	*N* accepted (*N* analysed)	Modern grains (%)	Overdispersion (%)	ulCAM (Gy)[1]	ulMAM3 (Gy)[2]	Residual dose (CAM – MAM D_e)	Total dose rate (Gy ka^{-1})[3]	ulCAM age (years)	ulMAM age (years)	Estimated true burial age (years)
BR001	Bar tail	43 (2400)	91	6	0.05±0.02	0.02±0.02	0.03±0.04	0.56±0.04	90±40	40±40	0–1
BR006	Bar tail	33 (1200)	91	<1	0.002±0.02	0.001±0.02	0.001±0.04	0.52±0.03	5±40	2±40	0–1
BR003	Mid-bar	52 (2600)	92	<1	0.08±0.03	0.04±0.016	0.04±0.036	0.64±0.04	110±40	50±30	0–1
BR004	Mid-bar	56 (1700)	95	<1	0.01±0.02	0.006±0.016	0.004±0.036	0.61±0.04	15±20	10±30	0–1
BR002	Floodplain bank	34 (1000)	79	90	0.16±0.02	0.07±0.03	0.09±0.05	0.56±0.03	280±50	120±50	>50
BR005	Floodplain top	33 (1400)	79	140	0.16±0.05	0.02±0.03	0.14±0.08	0.67±0.03	240±70	30±40	0–1
BR005MG	Floodplain top	24 (24)	62	130	0.32±0.09	0.07±0.03	0.25±0.12	0.67±0.03	480±140	100±50	0–1
BR007	Bar head	54 (2400)	81	73	0.13±0.02	0.09±0.02	0.04±0.04	0.52±0.03	250±50	170±40	~2–20
BR008	Bar head	45 (2400)	82	147	0.13±0.03	0.04±0.02	0.09±0.05	0.57±0.04	230±60	70±40	~2–20

[1]Unlogged central age model (Galbraith *et al.* 1999; Arnold *et al.* 2009).
[2]Unlogged minimum age model (Galbraith *et al.* 1999; Arnold *et al.* 2009).
[3]Dose rates were calculated using the conversion factors of Liritzis *et al.* (2013).

grains with non-zero ages are interpreted as grains that were not bleached during fluvial transport to the bar head and modern floodplain.

Dose distributions in these samples are indicative of partially bleached sediments (Fig. 6). Most grains cluster tightly around 0 Gy, reflecting the modern or near-modern depositional age of these sediments. However, this set of samples also has a wider variation of D_e values compared to samples from the mid-bar and bar tail depositional environments. A substantial number of grains in the bar head and floodplain samples exhibit D_e values exceeding 0.5 Gy, representing residual doses that were not bleached during the last transport event. For example, in BR007 25% of individual grain D_e values were >0.5 Gy, with one grain reaching 6.5 Gy.

Overdispersion values for the floodplain and bar head samples were consistently greater than 20%, ranging from 72 to 147% (Table 1). Minimum values of D_e for this group of samples are generally consistent with a zero dose ranging from 0.02±0.03 to 0.09±0.02 Gy. Central values of D_e for these samples are larger, ranging from 0.13±0.02 to 0.16±0.05 Gy. Residual doses for these samples are consistently larger than the four samples collected on the mid-bar and bar tail (ranging from 0.04±0.04 to 0.14±0.08 Gy; Table 1) and are up to seven times larger than the minimum D_e value.

Using the burial dose calculated with ul-CAM, calculated depositional ages for the floodplain and bar head samples range from 230±60 to 280±50 years. Including 2σ error on the calculated ages brings the range of minimum depositional ages to 110–180 years. Given that three out of four samples in this group have estimated depositional ages of <2 years to up to 20 years (samples BR005, BR007, BR008; Table 1), the depositional ages calculated using ul-CAM are likely significantly overestimated for these very young sediments. Overestimation of depositional ages using CAM commonly occurs in samples that were not well bleached prior to deposition (Olley *et al.* 1998, 2004; Wallinga 2002; Bailey & Arnold 2006; Arnold *et al.* 2007). Depositional ages calculated using ul-MAM are consistent with estimated true depositional ages for samples BR005 and BR008. The bar head sample BR007 yielded a depositional age of 170±40 years using ul-MAM, which is not consistent with the estimated true depositional age of 2–20 years (Fig. S4, Table S2).

Sample BR002 was collected from the exposed floodplain bank about 1.05 m below the floodplain surface. We estimate the true depositional age of this sample to be at least 50 years based on observations of mature trees on the floodplain surface (Fig. S2). The depositional age from ul-MAM was 120±50 years, which is consistent with our expectations of a non-zero depositional age for this sample. Comparison of the calculated minimum age with the significantly higher ul-CAM age (280±50 years) yields a residual age of 160±70 years and suggests that sediment collected in

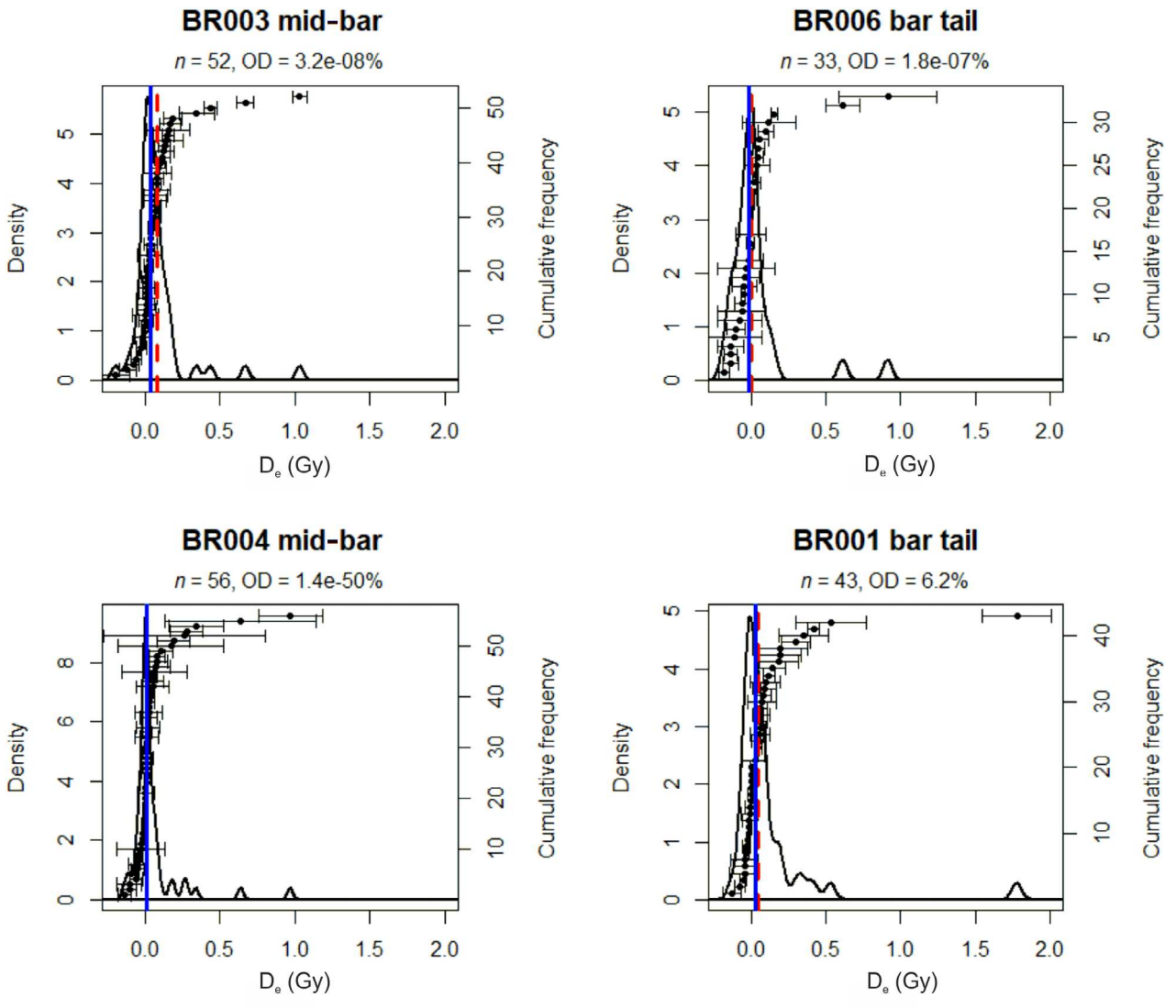

Fig. 5. D_e distributions for mid-bar and bar tail samples. The markers are D_e values of accepted grains plotted in rank order with standard error bars, and the solid black line is the kernel density estimate (KDE) of the D_e values. The solid blue line is the MAM D_e and the dashed red line is the CAM D_e.

this location was also incompletely bleached prior to deposition.

Multi-grain aliquots

Twenty-four multi-grain aliquots were analysed for the floodplain top sample (BR005). The dose distributions of multi-grain and single-grain aliquots appear similar. Most D_e values cluster around 0 Gy, with substantial tails of larger D_e values up to 1.55 Gy (Fig. 7). The multi-grain distribution also has one aliquot with a D_e value of 5 Gy, not shown in Fig. 7. The ul-MAM depositional ages of the multi-grain and single-grain aliquots were 100±50 and 30±40 years, respectively, consistent with each other within 1σ error. However, the ul-CAM depositional age from the multi-grain aliquots was 480±140 years, significantly higher than the ul-CAM age from single-grain aliquots (240±70 years). Both the multi-grain and single-grain samples of BR005 have significant residual doses (380 and 210 years, respectively) that were 3–7 times greater than the minimum dose, indicating partial bleaching prior to deposition (Chamberlain *et al*. 2018).

Dose rates

Dose rates for the modern floodplain samples were used to calculate depositional ages from the two different age models in order to better interpret deviation from the expected depositional age of 0 years for these modern sediments. Dose rates for the modern floodplain samples were relatively low when compared to dose rates from the adjacent terrace surface, ranging from 0.52±0.03 to 0.67±0.03 Gy ka^{-1} (Table 1) while terrace sediments

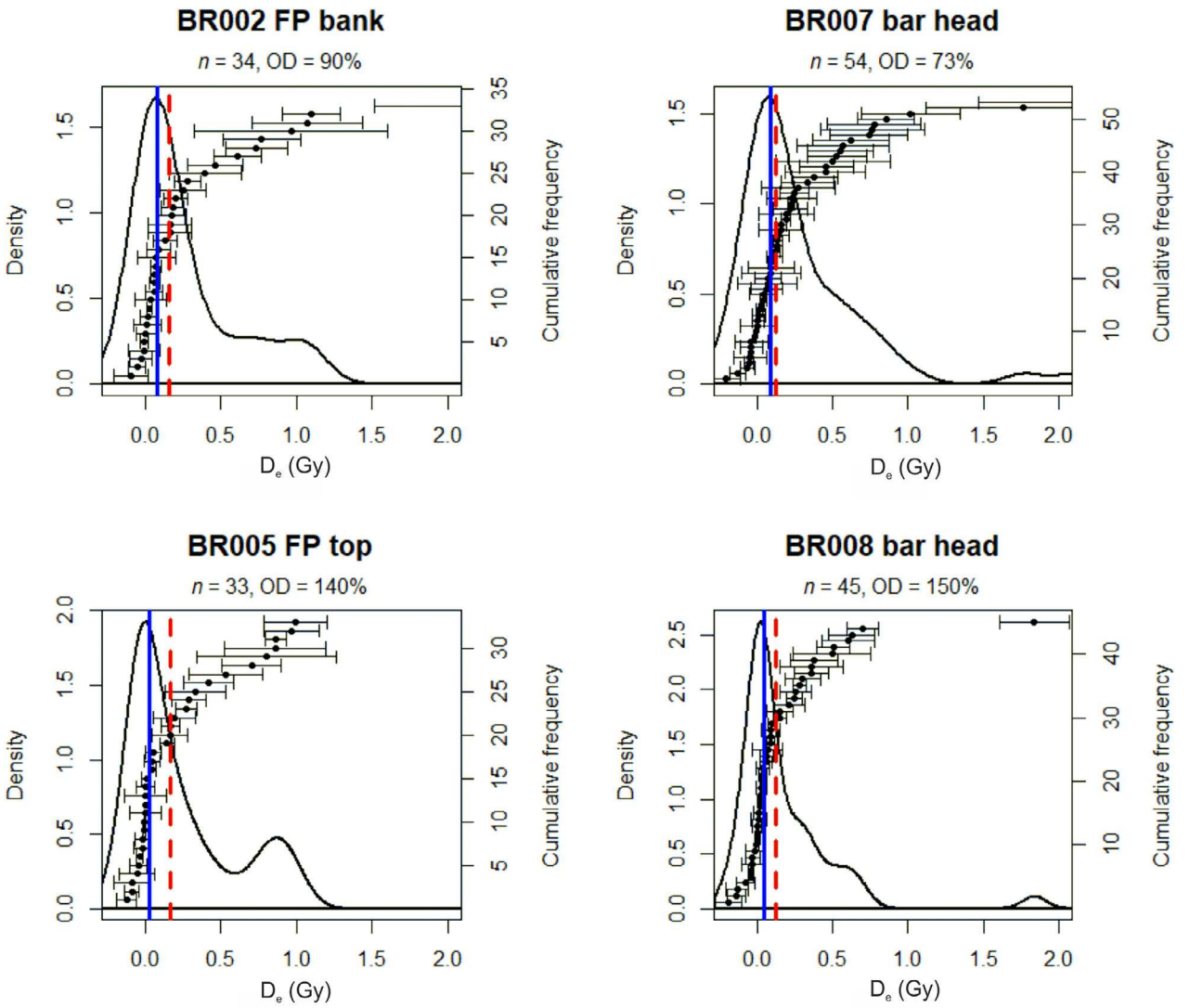

Fig. 6. D_e distributions for floodplain and bar head samples. The markers are D_e values of accepted grains plotted in rank order with standard error bars, and the solid black line is the kernel density estimate (KDE) of the D_e values. The solid blue line is the MAM D_e and the dashed red line is the CAM D_e.

had a calculated dose rates of 1.7±0.1 to 1.9±0.1 Gy ka^{-1} (Rodrigues *et al.* 2023) (Table 2). The lower dose rates for the modern floodplain may be due to the sampled sediments being composed of well-sorted quartz sands, as opposed to sediments collected from well-developed soils on the terrace surface. Terrace sediments likely include a higher proportion of clay- and silt-sized sediments that can bear radioactive minerals (Murray *et al.* 2021), resulting in a higher dose rate.

Comparison with terrace samples

These terrace sediments were analysed using single-grain quartz OSL, and the results were published in the primary publication Rodrigues *et al.* (2023). In this context, we present dose distributions from two terrace samples for comparison with modern samples. Rodrigues *et al.* (2023) used data from the modern floodplain samples presented here (BR002, BR005) as modern analogues to assess the degree of bleaching for the terrace samples. They concluded that the modern floodplain sediments were sufficiently well bleached to discount partial bleaching as the primary source of D_e scatter in their much older terrace samples. Due to the possibility of high beta dose heterogeneity, Rodrigues *et al.* (2023) used the average dose model (ADM), rather than CAM or MAM, to calculate equivalent dose (Guérin *et al.* 2017). We calculated equivalent doses for both terrace samples using ADM, CAM and MAM.

The equivalent doses for BUFF026 calculated using ADM (174±12 Gy) and CAM (166±12 Gy) overlap

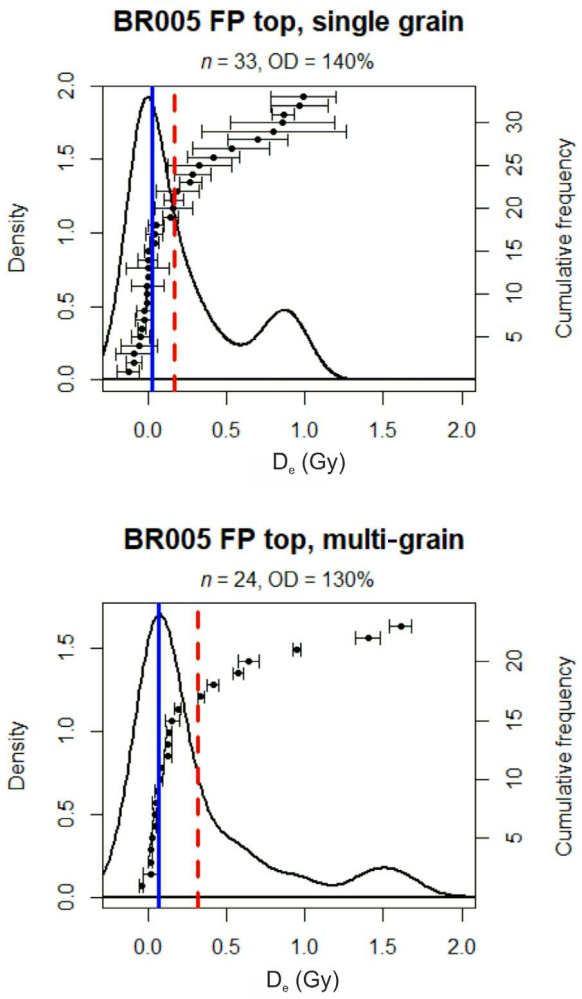

Fig. 7. D_e distribution for single-grain and multi-grain aliquots (4 mm) of the floodplain top sample (BR005). The markers are D_e values of accepted aliquots plotted in rank order with standard error bars, and the solid black line is the kernel density estimate (KDE) of the D_e values. The solid blue line is the MAM D_e and the dashed red line is the CAM D_e.

within 1σ; for completeness we also calculated the equivalent dose using MAM (126±19 Gy) (Table 2). The calculated residual dose (CAM-MAM) for BUFF026 is 40±31 Gy, a moderate residual dose that is only 32% of the MAM D_e. We estimate that the overwhelming majority, 90%, of individual grains in this sample were well bleached prior to deposition. The number of well-bleached grains, overdispersion value (25%), and relatively low residual dose suggest that most of the grains within sample BUFF026 were well bleached prior to deposition (Fig. 8, Table 2).

The equivalent doses for BUFF035 calculated using ADM (71±7 Gy) and CAM (62±6 Gy) overlap within 1σ, but the equivalent dose calculated using MAM is substantially lower at 28±4 Gy (Table 2). The overdispersion for BUFF035 is 51%, more typical of partially bleached sediments (Arnold & Roberts 2009). In

Table 2. OSL data and extended analysis of terrace samples from Rodrigues *et al.* (2023).

Sample number	Depositional environment	*N* accepted (*N* analysed)	Well-bleached grains (%)	Overdispersion (%)	ADM (Gy)[1]	CAM (Gy)[2]	MAM (Gy)[3]	Residual dose (CAM D_e – MAM D_e)	Total dose rate (Gy ka^{-1})[4]	CAM age (ka)	MAM age (ka)
BUFF026	Terrace	29 (4100)	90	25	174±12	166±12	126±19	40±22	1.7±0.1	95±8	72±11
BUFF035	Terrace	33 (2600)	33	51	71±7	62±6	28±4	34±7	1.9±0.1	32±3	14±2

[1]Average dose model (Guérin *et al.* 2017).
[2]Central age model (Galbraith *et al.* 1999).
[3]Minimum age model (Galbraith *et al.* 1999).
[4]Dose rates were calculated using the conversion factors of Liritzis *et al.* (2013) to one decimal place; ages were calculated using values prior to rounding. Dose rates were calculated assuming a water content of 10±6% (Rodrigues *et al.* 2023). External dose rates also include a cosmic dose component calculated according to Prescott & Hutton (1994). Total dose rates include an internal dose rate of 0.011±0.001 Gy ka^{-1}, which was calculated based on assumed internal U and Th concentrations provided by Rink & Odom (1991).

contrast to BUFF026, only 33% of individual grains in the BUFF039 sample were estimated to be well bleached prior to deposition (Table 2). A group of individual grains from this sample (11/33) clusters around the MAM equivalent dose (28±4 Gy) within 2σ, while the remaining grains exhibit D_e values ranging from 55 Gy up to 160 Gy (Fig. 8). The calculated residual dose for BUFF035 (34±7 Gy) is relatively large, more than 100% of the MAM equivalent dose (Chamberlain *et al.* 2018). The low number of well-bleached grains, overdispersion value, and substantial residual dose in sample BUFF035 appear characteristic of a sample that was partially bleached prior to deposition.

Discussion

Modern fluvial sediments often serve as analogues for estimating bleaching conditions at the time of deposition for older samples. However, the applicability of this analogue depends on accepting several critical underlying assumptions regarding depositional environment, river regime, sediment transport, and sediment sources. The first assumption is that the modern analogue sediment sample was taken from the same depositional environment as the older samples and that modern depositional environments are preserved in the depositional record. The second assumption is that the river had similar hydrological characteristics and sediment fluxes at the time of terrace sediment deposition compared to modern conditions (Olley *et al.* 2004; Arnold *et al.* 2007; Porat *et al.* 2010; Summa-Nelson & Rittenour 2012). The third assumption is that sources of sediment to the river channel were the same at the time of terrace deposition and modern sediment deposition (Gray & Mahan 2015; McGuire & Rhodes 2015b). We will discuss the implications of each of these assumptions individually and specifically related to our study site, then discuss implications for other rivers where modern samples are used to characterize bleaching conditions of older sediment deposits.

Influence of depositional environment

Our study reveals that even within a 125-m reach of a modern floodplain, there are subtle but discernible differences in bleaching characteristics across different depositional environments. At our field site, using only sediments from near-channel bars to characterize bleaching characteristics of sediments in the entire river would lead to the conclusion that modern fluvial sediments are uniformly well bleached, potentially masking partially bleached sediments on floodplains and in different reaches of the river. Thus, it is important to consider the likely depositional environment of palaeo-sediments when choosing the location on the modern floodplain to collect samples for characterization of bleaching.

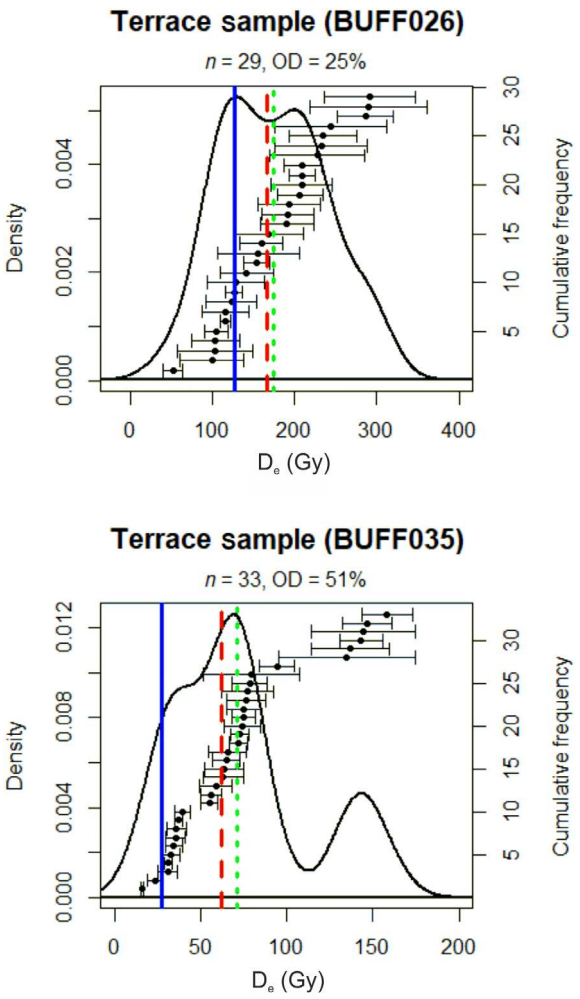

Fig. 8. D_e distributions for terrace samples from Rodrigues *et al.* (2023). The markers are D_e values of accepted aliquots plotted in rank order with standard error bars, and the solid black line is the kernel density estimate (KDE) of the D_e values. The solid blue line is the MAM D_e, the dashed red line is the CAM D_e, and the dotted green line is the ADM D_e.

The creation of specific depositional environments depends to a large extent on the river regime during the time of deposition, i.e. lateral migration, incision, or aggradation (Lewin & Macklin 2003). Sediments in terraces along the Buffalo River are characterized as overbank deposits (Rodrigues *et al.* 2023) and were deposited under a laterally migrating/aggrading river regime. Currently, the Buffalo River is incising into bedrock; thus, sediments preserved in neighbouring terraces may not be directly analogous to any sediments found on the relatively narrow modern floodplain.

The preservation potential of sediments in specific depositional environments also depends on the river regime (aggrading, incising, etc.). The two terrace samples were collected from overbank sand deposits that lacked stratigraphical structures such as ripples or cross-bedding that would suggest preservation of in-

channel sand deposits. However, given that cobble bar deposits are preserved in the terraces, it is likely that in-channel sand bars are also preserved, but not sampled. Sampling terrace sediments is likely biased towards thicker, homogenous packages of sandy overbank deposits that are both easier to sample from and to calculate dose rates. Despite the advantages of sampling massive sandy beds, some studies have suggested that they should be avoided for OSL sampling as they may have poorer bleaching characteristics compared to ripple laminated facies (Summa-Nelson & Rittenour 2012).

Effects of sediment and water flux on sediment bleaching

The second assumption for using modern analogues to assess bleaching in palaeo-sediments is that the river had similar hydrological characteristics and sediment fluxes at the time of terrace sediment deposition compared to modern conditions (Olley *et al*. 2004; Arnold *et al*. 2007; Porat *et al*. 2010; Tucker *et al*. 2011; Summa-Nelson & Rittenour 2012). Increased sediment flux to the river channel can cause a shift in river regime from incision to lateral migration by suppressing vertical incision and allowing lateral widening of the floodplain (Hancock & Anderson 2002; Johnson & Whipple 2010; Langston & Robertson 2023). Changes in sediment flux can also cause a change the river planform, for example from meandering to braided (e.g. Finnegan & Balco 2013). Shifts in river regime and shifts in river planform can result in vastly different depositional environments.

The sediments and terraces preserved along the Buffalo River indicate that the river underwent a long period of lateral bedrock widening and strath planation, followed by aggradation that lasted from 100 to 30 ka during the last glacial interval (Rodrigues *et al*. 2023). Following the end of the aggradational interval around 30 ka, the Buffalo River abandoned these terrace surfaces and rapidly incised through metres of sediment deposits and bedrock. Given that the modern Buffalo River is a vertically incising bedrock river, with only intermittent sediment cover on the bed, strath and fill terraces along the length of the river are evidence that the ratio of water and sediment flux used to be much higher in the past.

Changes in climate over glacial–interglacial cycles is the most likely driver of changes in water and sediment balance that caused the Buffalo River to shift from periods of valley widening and terrace formation to vertical incision and terrace abandonment (Bull 1990; Williams *et al*. 2006; Neudorf *et al*. 2014; Schanz *et al*. 2018; Bacon *et al*. 2023). Palaeoclimate records and global climate models in the south-central region of the USA point towards a climate that was substantially cooler and slightly wetter along the Buffalo River during glacial intervals (Dorale *et al*. 1998; Izumi & Bartlein 2016). Quantifying changes in discharge magnitude and frequency during the slightly wetter glacial periods is beyond the scope of this study; however, a link between warming temperatures and increasing precipitation intensity (Myhre *et al*. 2019) suggests that the Buffalo River watershed may have been wetter but less flashy during glacial intervals. On the other hand, the substantially cooler temperatures in the Buffalo River watershed during glacial intervals likely induced strong periglacial hillslope weathering (Marshall *et al*. 2021), which could have been a source of increased sediment flux to the river channels. Due to the relatively minor changes in precipitation in glacial intervals and the demonstrated importance of sediment cover in creating laterally mobile rivers (Langston & Robertson 2023), we hypothesize that changes in sediment flux were primarily responsible for the shift between lateral widening during terrace forming intervals and incision.

In addition to altering types of depositional environments, river channel planform, and different river regimes (incising vs. aggrading), changes in the water/sediment balance can impact sediment bleaching in transport. Increased sediment flux can increase turbidity in the water column, reducing sediment bleaching during transport (Gray & Mahan 2015; Mey *et al*. 2023). More sediment transported by the river also results in fewer sediment grains that are exposed and bleached at the surface, resulting in a partially bleached sediment package (Gray & Mahan 2015). Both factors could help explain why terrace samples and modern high-flow samples from the Buffalo River are apparently less well bleached than modern in-channel sediments.

A shift to a flashier discharge regime tends to encourage vertical incision (Tucker 2004) and can potentially result in less complete bleaching of sediments in the river (Gray & Mahan 2015). Relationships between river discharge and sediment luminescence signals have been demonstrated by several studies. In semi-arid regions, episodic transport of sediment during high-flow stages prevents full bleaching of sediment during rapid transport events (Porat *et al*. 2001; Gray & Mahan 2015; McGuire & Rhodes 2015b). Sediments that are frequently reworked by the river tend to be better bleached than infrequently reworked sediments and flood deposits (King *et al*. 2014b; Cunningham *et al*. 2015a). If changes in sediment flux or water discharge are invoked as the cause for shifts in widening vs. incising intervals, we must also acknowledge the likelihood that terrace deposits were not deposited under the same flow conditions as the current incising interval.

Sediment sources

The third assumption is that sources of sediment to the river channel were the same at the time of terrace deposition and modern sediment deposition (Gray & Mahan 2015; McGuire & Rhodes 2015b). Changes in sediment sources through time are likely, particularly if the river alternates between periods of stability and

incision (Bonnet *et al.* 2019; Guyez *et al.* 2022). Sediment grains eroded from ancient floodplains or directly from bedrock often contain grains with high palaeodoses or even saturated grains, contributing to sediments with significant partial bleaching at the time of burial (Robertson *et al.* 2022).

While we do not know if or how sediment sources have varied through time in the Buffalo River, variation in sediment sources is certainly possible or even likely. Sediments in the river can be sourced from upstream, local terrace or floodplain erosion, local bedrock erosion, or from hillslope inputs. Given the likelihood of increased sediment flux from hillslopes to the river channels during glacial intervals, it is possible that sediments stored in terraces along the Buffalo are enriched with sediments sourced from hillslopes. Hillslope sediments often have much larger residual doses than fluvially transported sediment (Gray *et al.* 2022), which could contribute to the apparent partial bleaching in some Buffalo River terrace sediments.

Implications for other rivers

Many studies rely on modern analogues to assess the degree of bleaching in ancient terrace sediments. Our findings emphasize the importance of certain assumptions that we make when using modern sediments to characterize bleaching conditions of ancient sediments. If we assume that ancient terrace sediments experienced the same bleaching history as their modern fluvial counterparts, we must also accept several underlying assumptions, including the similarity of the depositional environment, hydrological regime of the river, sediment transport in the river, and sediment sources between modern and ancient samples.

Our study highlights that the bleaching characteristics of modern samples can significantly influence the choice of age model for palaeo-deposits. Therefore, when confronted with modern floodplain sediments that exhibit relatively good bleaching characteristics alongside D_e distributions in older sediment deposits that are reminiscent of partially bleached samples, researchers must exercise caution in selecting the appropriate age model. Selecting an inappropriate age model when dating older fluvial sediments can result in an inaccurate determination of age, which has important implications for correctly interpreting climate-driven fluvial regimes in the past and calculating rates of landscape evolution based on luminescence dating, e.g. bedrock incision rates from strath terraces (Foster *et al.* 2017). Our results underscore the need for careful evaluation of partial bleaching, beta dose heterogeneity, postdepositional mixing, or potentially all three in unknown contributions (Smedley *et al.* 2020) as significant sources of scatter in dose distributions.

Our results challenge the widely held assumption that modern fluvial sediments represent the worst possible scenario for sediment bleaching (Jain *et al.* 2004; Murray *et al.* 2012; McGuire & Rhodes 2015b). Partially bleached fluvial sediments from modern environments have been documented in a wide range of rivers with varying flow regime, planforms, and depositional environments (Stokes *et al.* 2001; Olley *et al.* 2004; Sim *et al.* 2014; Gliganic *et al.* 2017; Larkin *et al.* 2017; Rizza *et al.* 2024). In contrast, our results show that sediments from in-channel bars were well bleached and had very few grains with even small residual doses. Our results are consistent with previous work that has found that longer transport distances, longer time spent on a depositional surface, and lower flow regimes tend to result in more well-bleached sediment samples (Porat *et al.* 2001; Stokes *et al.* 2001; Cunningham *et al.* 2015a, b; Gray & Mahan 2015; McGuire & Rhodes 2015b; Gliganic *et al.* 2017).

Our results also demonstrate that pairs of samples from the same depositional environments and even samples across similar depositional environments have very similar bleaching characteristics. Our three pairs of repeat sample measurements allow us to more confidently attribute bleaching characteristics of depositional environment to physical processes rather than statistical noise (Cunningham *et al.* 2015b). The similarity of bleaching characteristics in our sample groups is in contrast to other work that has shown substantial variability in dose distributions of modern sediments that are only tens of centimetres apart (e.g. Rizza *et al.* 2024). In the case of the Severaisse River, a high elevation braided river, significant sediment contributions from slope mass failures and short transport distances from the parent bedrock to the river likely resulted in significant residual doses in modern sediments (Rizza *et al.* 2024). In contrast, the transport distance for fluvial sediments at our site is likely tens of kilometres (Fig. 2), allowing ample opportunity for sediment bleaching during transport or while exposed at the surface of bars between flood events. The lesson we can take away from the wide variation in bleaching characteristics of fluvial sediments is that sediment bleaching in fluvial environments is highly variable and depends on the particular river, specific sediment characteristics and sources, and depositional environment.

Interpreting dose distributions and bleaching characteristics of sediments with the goal of interpreting past depositional environments and geomorphic processes is promising, but still in the early phases of development. Making strong correlations with bleaching characteristics and depositional environment and geomorphic processes will remain challenging wherever the degree of bleaching is highly time and space dependent (Chamberlain & Wallinga 2019; Rizza *et al.* 2024). While some studies have correlated bleaching characteristics with depositional environment or flow regime (King *et al.* 2014b; Cunningham *et al.* 2015a), others have shown that bleaching characteristics within depositional environments can vary widely and without obvious

explanation for the variations (Cunningham *et al*. 2015b; Chamberlain & Wallinga 2019). Bleaching characteristics of sediments are controlled in part by the suite of geomorphic processes that they have undergone prior to deposition. It is critical to understand and refine the relationships between sediment bleaching characteristics and geomorphic processes in modern sediments before we can use palaeo-deposits to make interpretations about geomorphic processes that were active in the past. Characterizing luminescence signals in sediments at a single location during different flow stages is a promising direction for future research. Such data would help quantify how sediment bleaching characteristics vary through time and with transport process and potentially explain why bleaching within a single depositional environment location can be so variable.

Influence of beta dose heterogeneity

The accuracy and precision of OSL ages are highly dependent upon the choice of age model (e.g. MAM vs. CAM vs. ADM) used to calculate the depositional age. The selection of an age model depends on the interpretation of sources of scatter in the dose distribution. Scatter in dose distributions can be the result of partial bleaching, beta dose heterogeneity, postdepositional mixing, or a combination of all three. Unfortunately, currently there are no models that can analyse samples with both partial bleaching and beta dose heterogeneity (Murray *et al*. 2021), and more importantly, there is no systematic method to determine the contribution of partial bleaching vs. beta dose heterogeneity to scatter in dose distributions. Studies have suggested that beta dose rates are more heterogeneous at overall low dose rates (<1 Gy ka^{-1}), primarily due to low concentration of radiogenic elements K, U, Th (Mayya *et al*. 2006; Guérin *et al*. 2015; Jankowski & Jacobs 2018; Smedley *et al*. 2020), but empirical assessment of beta dose heterogeneity is difficult and time consuming. Recent empirical studies on quantifying heterogeneity in beta dose have found that it explained some, but not all, scatter in the study sample dose distributions (Jankowski & Jacobs 2018; Smedley *et al*. 2020). Thus, the authors of these studies recommend that the beta dosimetric environment be characterized before scatter in dose distributions is attributed to beta dose heterogeneity.

In our study, low K concentrations in the terrace sediments adjacent to our study site suggest that these sediments may have been influenced by beta dose heterogeneity. While the modern floodplain sediments are generally well bleached, the terrace sediments were likely deposited under a different fluvial regime compared to modern fluvial conditions making it difficult to rule out partial bleaching as a source of D_e scatter. The uncertainty surrounding the origin of scatter in dose distributions highlights the importance of developing an age model that accounts for both partial bleaching and beta dose heterogeneity and the need for more research to characterize sources of scatter in dose distributions.

Conclusions

We have shown that even within a small area of a modern floodplain along the Buffalo River in northwest Arkansas, USA, there can be variations in bleaching characteristics across different depositional environments. Analysis of sediment samples collected from distinct depositional environments on the modern floodplain reveal subtle yet distinguishable differences in the dose distributions of these modern sediment samples, depending on their depositional environment. Samples from mid-bar and bar tail locations show fully bleached sediments, while those from the floodplain and areas with interbedded cobbles exhibit signs of partial bleaching during transport and likely deposition during high-flow events. The significance of this work extends beyond the identification of different D_e distributions within varying depositional environments. Our results also challenge the conventional expectation that modern fluvial sediments reflect a worst-case bleaching scenario.

Many studies rely on modern analogues to assess the degree of bleaching in ancient terrace sediments. Our study highlights that the bleaching characteristics of modern samples can significantly influence the choice of age model for palaeo-deposits. Therefore, when confronted with modern floodplain sediments that exhibit relatively good bleaching characteristics alongside D_e distributions in older sediment deposits that are reminiscent of partially bleached samples, researchers must exercise caution in selecting the appropriate age model. Our results underscore the need for careful evaluation of the origin of scatter in dose distributions in order to avoid overlooking beta dose heterogeneity and postdepositional mixing as significant sources of D_e scatter.

Our findings also emphasize the importance of certain assumptions that we make when using modern sediments to characterize bleaching conditions of ancient sediments. If we assume that ancient terrace sediments experienced the same bleaching history as their modern fluvial counterparts, we must also accept several underlying assumptions. These assumptions include the similarity of the depositional environment, hydrological regime of the river, sediment transport in the river, and sediment sources between modern and ancient samples. Since changes in sediment flux and water discharge regime over time are often cited as a driver of fluvial terrace formation, we should not neglect how these changes could affect sediment bleaching conditions. While modern sediments may not act as perfect analogues for estimating bleaching conditions in older sediments, particularly in fluvial terrace settings, they can help researchers gain important insight into potential sources of D_e scatter.

Acknowledgements. – The Desert Research Institute Luminescence Laboratory is gratefully acknowledged for hosting ALL and ALM to undertake and complete this work. We would like to acknowledge funding from NSF grant OIA-1833025 and NSF grant EAR-2051559. We thank two anonymous reviewers for their thoughtful comments that greatly improved this manuscript.

Author contributions. – ALL acquired funding for this study. ALL and AK-Z conceptualized this study. ALL, AK-Z and ALM collected the samples analysed in this study and CMN, ALL and ALM analysed the samples. All authors contributed to conceptualizing and writing the manuscript.

Data availability statement. – Data used in this manuscript can be accessed at: https://github.com/alangston/modernBR_floodplain.

References

Aitken, M. J. 1982: Thermoluminescence dating: past progress and future trends. *Nuclear Tracks and Radiation Measurements 10*, 3–6.

Aitken, M. J. 1985: *Thermoluminescence Dating*. 351 pp. Academic Press, London.

Aitken, M. J. & Smith, B. W. 1988: Optical dating: recuperation after bleaching. *Quaternary Science Reviews 7*, 387–393.

Alexanderson, H. & Murray, A. S. 2012: Luminescence signals from modern sediments in a glaciated bay, NW Svalbard. *Quaternary Geochronology 10*, 250–256.

Arnold, L. J. & Roberts, R. G. 2009: Stochastic modelling of multi-grain equivalent dose (De) distributions: implications for OSL dating of sediment mixtures. *Quaternary Geochronology 4*, 204–230.

Arnold, L. J., Bailey, R. M. & Tucker, G. E. 2007: Statistical treatment of fluvial dose distributions from southern Colorado arroyo deposits. *Quaternary Geochronology 2*, 162–167.

Arnold, L. J., Demuro, M., Spooner, N. A., Prideaux, G. J., McDowell, M. C., Camens, A. B., Reed, E. H., Parés, J. M., Arsuaga, J. L., Bermúdez de Castro, J. M. & Carbonell, E. 2019: Single-grain TT-OSL bleaching characteristics: insights from modern analogues and OSL dating comparisons. *Quaternary Geochronology 49*, 45–51.

Arnold, L. J., Roberts, R. G., Galbraith, R. F. & DeLong, S. B. 2009: A revised burial dose estimation procedure for optical dating of young and modern-age sediments. *Quaternary Geochronology 4*, 306–325.

Bacon, S. N., Bullard, T. F., Kimball, V., Neudorf, C. M. & Baker, S. A. 2023: Landscape response to hydroclimate variability shown by the post-Bonneville Flood (ca. 18 ka) fluvial-geomorphic history of the middle Snake River, Idaho, USA. *Quaternary Research 113*, 29–51.

Bailey, R. M. & Arnold, L. J. 2006: Statistical modelling of single grain quartz De distributions and an assessment of procedures for estimating burial dose. *Quaternary Science Reviews 25*, 2475–2502.

Bateman, M. D., Boulter, C. H., Carr, A. S., Frederick, C. D., Peter, D. & Wilder, M. 2007: Preserving the palaeoenvironmental record in drylands: bioturbation and its significance for luminescence-derived chronologies. *Sedimentary Geology 195*, 5–19.

Bateman, M. D., Frederick, C. D., Jaiswal, M. K. & Singhvi, A. K. 2003: Investigations into the potential effects of pedoturbation on luminescence dating. *Quaternary Science Reviews 22*, 1169–1176.

Bonnet, S., Reimann, T., Wallinga, J., Lague, D., Davy, P. & Lacoste, A. 2019: Landscape dynamics revealed by luminescence signals of feldspars from fluvial terraces. *Scientific Reports 9*, 1–9.

Braden, A. K. & Ausbrooks, S. M. 2003: *Geologic map of the Mt. Judea Quadrangle, Newton County, Arkansas. Arkansas Geological Commission, Digital Geologic Quadrangle Map DGM-AR-00590: 1:24,000 scale.*

Brown, N. D. 2020: Which geomorphic processes can be informed by luminescence measurements? *Geomorphology 367*, 107296, https://doi.org/10.1016/j.geomorph.2020.107296.

Bull, W. B. 1990: Stream-terrace genesis: implications for soil development. *Geomorphology 3*, 351–367.

Chamberlain, E. L. & Wallinga, J. 2019: Seeking enlightenment of fluvial sediment pathways by optically stimulated luminescence signal bleaching of river sediments and deltaic deposits. *Earth Surface Dynamics 7*, 723–736.

Chamberlain, E. L., Wallinga, J. & Shen, Z. 2018: Luminescence age modeling of variably-bleached sediment: model selection and input. *Radiation Measurements 120*, 221–227.

Cunningham, A. C., Evans, M. & Knight, J. 2015a: Quantifying bleaching for zero-age fluvial sediment: a Bayesian approach. *Radiation Measurements 81*, 55–61.

Cunningham, A. C., Wallinga, J., Hobo, N., Versendaal, A. J., Makaske, B. & Middelkoop, H. 2015b: Re-evaluating luminescence burial doses and bleaching of fluvial deposits using Bayesian computational statistics. *Earth Surface Dynamics 3*, 55–65.

Dorale, J. A., Edwards, R. L., Ito, E. & Gonzalez, L. A. 1998: Climate and vegetation history of the midcontinent from 75 to 25 ka: a speleothem record from Crevice Cave, Missouri, USA. *Science 282*, 1871–1874.

Duller, G. A. T. 2004: Luminescence dating of Quaternary sediments: recent advances. *Journal of Quaternary Science 19*, 183–192.

Duller, G. A. T. 2008: Single-grain optical dating of Quaternary sediments: why aliquot size matters in luminescence dating. *Boreas 37*, 589–612.

Duller, G. A. T. 2018: *Analyst v4.56. User Manual*. 111 pp. Aberystwyth University, Aberystwyth.

Durcan, J. A., King, G. E. & Duller, G. A. T. 2015: DRAC: Dose Rate and Age Calculator for trapped charge dating. *Quaternary Geochronology 28*, 54–61.

Feathers, J. K. 2003: Single-grain OSL dating of sediments from the Southern High Plains, USA. *Quaternary Science Reviews 22*, 1035–1042.

Finnegan, N. J. & Balco, G. 2013: Sediment supply, base level, braiding, and bedrock river terrace formation: Arroyo Seco, California, USA. *Geological Society of America Bulletin 125*, 1114–1124.

Foster, M. A., Anderson, R. S., Gray, H. J. & Mahan, S. A. 2017: Dating of river terraces along Lefthand Creek, western High Plains, Colorado, reveals punctuated incision. *Geomorphology 295*, 176–190.

Galbraith, R. F. & Roberts, R. G. 2012: Statistical aspects of equivalent dose and error calculation and display in OSL dating: an overview and some recommendations. *Quaternary Geochronology 11*, 1–27.

Galbraith, R. F., Roberts, R. G., Laslett, G. M., Yoshida, H. & Olley, J. M. 1999: Optical dating of single and multiple grains of quartz from Jinmium rock shelter, northern Australia: part I, experimental design and statistical models. *Archaeometry 41*, 339–364.

Gliganic, L. A., Cohen, T. J., Meyer, M. & Molenaar, A. 2017: Variations in luminescence properties of quartz and feldspar from modern fluvial sediments in three rivers. *Quaternary Geochronology 41*, 70–82.

Gliganic, L. A., Cohen, T. J., Slack, M. & Feathers, J. K. 2016: Sediment mixing in aeolian sandsheets identified and quantified using single-grain optically stimulated luminescence. *Quaternary Geochronology 32*, 53–66.

Godfrey-Smith, D. I., Huntley, D. J. & Chen, W. H. 1988: Optical dating studies of quartz and feldspar sediment extracts. *Quaternary Science Reviews 7*, 373–380.

Gray, H. J. & Mahan, S. A. 2015: Variables and potential models for the bleaching of luminescence signals in fluvial environments. *Quaternary International 362*, 42–49.

Gray, H. J., DuRoss, C., Nicovich, S. & Gold, R. 2022: Luminescence sediment tracing reveals the complex dynamics of colluvial wedge formation. *Science Advances 8*, 1–12.

Gray, H. J., Jain, M., Sawakuchi, A. O., Mahan, S. A. & Tucker, G. E. 2019: Luminescence as a sediment tracer and provenance tool. *Reviews of Geophysics 57*, 987–1017.

Gray, H. J., Tucker, G. E., Mahan, S. A., McGuire, C. & Rhodes, E. J. 2017: On extracting sediment transport information from measurements of luminescence in river sediment. *Journal of Geophysical Research: Earth Surface 122*, 654–677.

Guérin, G., Christophe, C., Philippe, A., Murray, A. S., Thomsen, K. J., Tribolo, C., Urbanova, P., Jain, M., Guibert, P., Mercier, N., Kreutzer, S. & Lahaye, C. 2017: Absorbed dose, equivalent dose,

measured dose rates, and implications for OSL age estimates: introducing the Average Dose Model. *Quaternary Geochronology 41*, 163–173.
Guérin, G., Jain, M., Thomsen, K. J., Murray, A. S. & Mercier, N. 2015: Modelling dose rate to single grains of quartz in well-sorted sand samples: the dispersion arising from the presence of potassium feldspars and implications for single grain OSL dating. *Quaternary Geochronology 27*, 52–65.
Guérin, G., Mercier, N., Nathan, R., Adamiec, G. & Lefrais, Y. 2012: On the use of the infinite matrix assumption and associated concepts: a critical review. *Radiation Measurements 47*, 778–785.
Guyez, A., Bonnet, S., Reimann, T., Carretier, S. & Wallinga, J. 2022: Illuminating past river incision, sediment source and pathways using luminescence signals of individual feldspar grains (Rangitikei River, New Zealand). *Earth Surface Processes and Landforms 47*, 1952–1971.
Guyez, A., Bonnet, S., Reimann, T., Carretier, S. & Wallinga, J. 2023: A novel approach to quantify sediment transfer and storage in rivers—testing feldspar single-grain pIRIR analysis and numerical simulations. *Journal of Geophysical Research: Earth Surface 128*, 1–21.
Hancock, G. S. & Anderson, R. S. 2002: Numerical modeling of fluvial strath-terrace formation in response to oscillating climate. *Geological Society of America Bulletin 114*, 1131–1142.
Hu, G., Zhang, J. F., Qiu, W. L. & Zhou, L. P. 2010: Residual OSL signals in modern fluvial sediments from the Yellow River (HuangHe) and the implications for dating young sediments. *Quaternary Geochronology 5*, 187–193.
Izumi, K. & Bartlein, P. J. 2016: North American paleoclimate reconstructions for the Last Glacial Maximum using an inverse modeling through iterative forward modeling approach applied to pollen data. *Geophysical Research Letters 43*, 10965–10972.
Jacobs, Z., Wintle, A. G., Roberts, R. G. & Duller, G. A. T. 2008: Equivalent dose distributions from single grains of quartz at Sibudu, South Africa: context, causes and consequences for optical dating of archaeological deposits. *Journal of Archaeological Science 35*, 1808–1820.
Jain, M., Murray, A. S. & Bøtter-Jensen, L. 2004: Optically stimulated luminescence dating: how significant is incomplete light exposure in fluvial environments? *Quaternaire 15*, 143–157.
Jankowski, N. R. & Jacobs, Z. 2018: Beta dose variability and its spatial contextualisation in samples used for optical dating: an empirical approach to examining beta microdosimetry. *Quaternary Geochronology 44*, 23–37.
Johnson, J. P. L. & Whipple, K. X. 2010: Evaluating the controls of shear stress, sediment supply, alluvial cover, and channel morphology on experimental bedrock incision rate. *Journal of Geophysical Research: Earth Surface (2003–2012) 115*, F02018, https://doi.org/10.1029/2009JF001335.
Keen-Zebert, A., Hudson, M. R., Shepherd, S. L. & Thaler, E. A. 2017: The effect of lithology on valley width, terrace distribution, and bedload provenance in a tectonically stable catchment with flat-lying stratigraphy. *Earth Surface Processes and Landforms 42*, 1573–1587.
King, G. E., Robinson, R. A. J. & Finch, A. A. 2013: Apparent OSL ages of modern deposits from Fåbergstølsdalen, Norway: implications for sampling glacial sediments. *Journal of Quaternary Science 28*, 673–682.
King, G. E., Robinson, R. A. J. & Finch, A. A. 2014a: Towards successful OSL sampling strategies in glacial environments: deciphering the influence of depositional processes on bleaching of modern glacial sediments from Jostedalen, southern Norway. *Quaternary Science Reviews 89*, 94–107.
King, G. E., Sanderson, D. C. W., Robinson, R. A. J. & Finch, A. A. 2014b: Understanding processes of sediment bleaching in glacial settings using a portable OSL reader. *Boreas 43*, 955–972.
Kreutzer, S., Burow, C., Dietze, M., Fuchs, M. C., Schmidt, C., Fischer, M., Friedrich, J., Mercier, N., Philippe, A., Riedesel, S., Autzen, M., Mittelstrass, D., Gray, H. J. & Galharret, J. 2023: *Luminescence: Comprehensive Luminescence Dating Data Analysis*. 359 pp. Package. Available at: https://r-lum.github.io/Luminescence/.
Kristensen, J. A., Thomsen, K. J., Murray, A. S., Buylaert, J. P., Jain, M. & Breuning-Madsen, H. 2015: Quantification of termite bioturbation in a savannah ecosystem: application of OSL dating. *Quaternary Geochronology 30*, 334–341.
Langston, A. L. & Robertson, C. H. 2023: Wide bedrock valley development and sensitivity to environmental perturbations: insights from flume experiments in erodible bedrock. *Earth Surface Processes and Landforms 48*, 3041–3058.
Larkin, Z. T., Tooth, S., Ralph, T. J., Duller, G. A. T., McCarthy, T., Keen-Zebert, A. & Humphries, M. S. 2017: Timescales, mechanisms, and controls of incisional avulsions in floodplain wetlands: insights from the Tshwane River, semiarid South Africa. *Geomorphology 283*, 158–172.
Lewin, J. & Macklin, M. G. 2003: Preservation potential for late Quaternary river alluvium. *Journal of Quaternary Science 18*, 107–120.
Li, Z., Gao, S., Chen, M., Zhang, J., Gourley, J. J., Wen, Y., Yang, T. & Hong, Y. 2023: Introducing flashiness-intensity-duration-frequency (F-IDF): a new metric to quantify flash flood intensity. *Geophysical Research Letters 50*, e2023GL104992, https://doi.org/10.1029/2023GL104992.
Liritzis, I., Stamoulis, K. C., Papachristodoulou, C. & Ionnides, K. 2013: A re-evaluation of radiation dose-rate conversion factors. *Mediterranean Archaeology and Archaeometry 13*, 1–15.
Madsen, A. T. & Murray, A. S. 2009: Optically stimulated luminescence dating of young sediments: a review. *Geomorphology 109*, 3–16.
Marshall, J. A., Roering, J. J., Rempel, A. W., Shafer, S. L. & Bartlein, P. J. 2021: Extensive frost weathering across unglaciated North America during the Last Glacial Maximum. *Geophysical Research Letters 48*, e2020GL090305, https://doi.org/10.1029/2020GL090305.
Mayya, Y. S., Morthekai, P., Murari, M. K. & Singhvi, A. K. 2006: Towards quantifying beta microdosimetric effects in single-grain quartz dose distribution. *Radiation Measurements 41*, 1032–1039.
McGuire, C. & Rhodes, E. J. 2015a: Determining fluvial sediment virtual velocity on the Mojave River using K-feldspar IRSL: initial assessment. *Quaternary International 362*, 124–131.
McGuire, C. & Rhodes, E. J. 2015b: Downstream MET-IRSL single-grain distributions in the Mojave River, southern California: testing assumptions of a virtual velocity model. *Quaternary Geochronology 30*, 239–244.
Mey, J., Schwanghart, W., De Boer, A. M. & Reimann, T. 2023: Differential bleaching of quartz and feldspar luminescence signals under high-turbidity conditions. *Geochronology 5*, 377–389.
Murray, A. S. 1996: Developments in optically stimulated luminescence and photo-transferred thermoluminescence dating of young sediments: application to a 2000-year sequence of flood deposits. *Geochimica et Cosmochimica Acta 60*, 565–576.
Murray, A. S., Arnold, L. J., Buylaert, J. P., Guérin, G., Qin, J., Singhvi, A. K., Smedley, R. & Thomsen, K. J. 2021: Optically stimulated luminescence dating using quartz. *DTU Orbit 1*, 72, https://doi.org/10.1038/s43586-021-00068-5.
Murray, A. S., Thomsen, K. J., Masuda, N., Buylaert, J. P. & Jain, M. 2012: Identifying well-bleached quartz using the different bleaching rates of quartz and feldspar luminescence signals. *Radiation Measurements 47*, 688–695.
Murray, A. S. & Wintle, A. G. 2000: Luminescence dating of quartz using an improved single-aliquot regenerative-dose protocol. *Radiation Measurements 32* (1), 57–73.
Myhre, G., Alterskjær, K., Stjern, C. W., Hodnebrog, Ø., Marelle, L., Samset, B. H., Sillmann, J., Schaller, N., Fischer, E., Schulz, M. & Stohl, A. 2019: Frequency of extreme precipitation increases extensively with event rareness under global warming. *Scientific Reports 9*, 1–10.
Nathan, R. P., Thomas, P. J., Jain, M., Murray, A. S. & Rhodes, E. J. 2003: Environmental dose rate heterogeneity of beta radiation and its implications for luminescence dating: Monte Carlo modelling and experimental validation. *Radiation Measurements 37*, 305–313.
Neely, B. L. 1985: The flood of December 1982 and the 100- and 500-year flood on the Buffalo River, Arkansas. *U.S. Geological Survey Water-Resources Investigations Report 85-4192*, 37 pp.
Neudorf, C. M., Roberts, R. G. & Jacobs, Z. 2014: Testing a model of alluvial deposition in the Middle Son Valley, Madhya Pradesh, India—IRSL dating of terraced alluvial sediments and implications for

archaeological surveys and palaeoclimatic reconstructions. *Quaternary Science Reviews 89*, 56–69.
Olley, J. M., Caitcheon, G. & Murray, A. 1998: The distribution of apparent dose as determined by optically stimulated luminescence in small aliquots of fluvial quartz: implications for dating young sediments. *Quaternary Science Reviews 17*, 1033–1040.
Olley, J. M., Pietsch, T. & Roberts, R. G. 2004: Optical dating of Holocene sediments from a variety of geomorphic settings using single grains of quartz. *Geomorphology 60*, 337–358.
Olley, J. M., Roberts, R. G. & Murray, A. S. 1997: Disequilibria in the uranium decay series in sedimentary deposits at Allen's Cave, Nullarbor Plain, Australia: implications for dose rate determinations. *Radiation Measurements 27*, 433–443.
Porat, N., Amit, R., Enzel, Y., Zilberman, E., Avni, Y., Ginat, H. & Gluck, D. 2010: Abandonment ages of alluvial landforms in the hyperarid Negev determined by luminescence dating. *Journal of Arid Environments 74*, 861–869.
Porat, N., Zilberman, E., Amit, R. & Enzel, Y. 2001: Residual ages of modern sediments in an hyperarid region, Israel. *Quaternary Science Reviews 20*, 795–798.
Prescott, J. R. & Hutton, J. T. 1994: Cosmic ray contributions to dose rates for luminescence and ESR dating: large depths and long-term time variations. *Radiation Measurements 23* (2-3), 497–500.
Rajapara, H. M., Kumar, V., Chauhan, N., Gajjar, P. N. & Singhvi, A. K. 2020: Bleaching of blue light stimulated luminescence of quartz by moonlight. *Journal of Earth System Science 129*, 212, https://doi.org/10.1007/s12040-020-01474-1.
Reimann, T., Román-Sánchez, A., Vanwalleghem, T. & Wallinga, J. 2017: Getting a grip on soil reworking – single-grain feldspar luminescence as a novel tool to quantify soil reworking rates. *Quaternary Geochronology 42*, 1–14.
Rink, W. J. & Odom, A. L. 1991: Natural alpha recoil particle radiation and ionizing radiation sensitivities in quartz detected with EPR: implications for geochronometry. *International Journal of Radiation Applications and Instrumentation. 18* (1-2), 163–173.
Rittenour, T. M. 2008: Luminescence dating of fluvial deposits: applications to geomorphic, palaeoseismic and archaeological research. *Boreas 37*, 613–635.
Rizza, M., Rixhon, G., Valla, P. G., Gairoard, S., Delanghe, D., Fleury, J., Tal, M. & Groleau, S. 2024: Revisiting a proof of concept in quartz-OSL bleaching processes using sands from a modern-day river (the Séveraisse, French Alps). *Quaternary Geochronology 82*, 101520, https://doi.org/10.1016/j.quageo.2024.101520.
Roberts, R. G., Galbraith, R. F., Yoshida, H., Laslett, G. M. & Olley, J. M. 2000: Distinguishing dose populations in sediment mixtures: a test of single-grain optical dating procedures using mixtures of laboratory-dosed quartz. *Radiation Measurements 32*, 459–465.
Robertson, C. H., Neudorf, C. M. & Langston, A. L. 2022: The Role of Talus Piles on the Genesis of Wide Bedrock Valleys: Using Optically Stimulated Luminescence to Estimate the Residence Times of Talus Blocks in Wide and Narrow Bedrock Valleys. *American Geophysical Union Annual Meeting, Chicago, IL*.
Rodrigues, K., Keen-Zebert, A., Shepherd, S., Hudson, M. R., Bitting, C. J., Johnson, B. G. & Langston, A. 2023: The role of lithology and climate on bedrock river incision and terrace development along the Buffalo National River, Arkansas. *Quaternary Research 32*, 179–193.
Román-Sánchez, A., Reimann, T., Wallinga, J. & Vanwalleghem, T. 2019: Bioturbation and erosion rates along the soil-hillslope conveyor belt, part 1: insights from single-grain feldspar luminescence. *Earth Surface Processes and Landforms 44*, 2051–2065.
Schanz, S. A., Montgomery, D. R., Collins, B. D. & Duvall, A. R. 2018: Multiple paths to straths: a review and reassessment of terrace genesis. *Geomorphology 312*, 12–23.
Sim, A. K., Thomsen, K. J., Murray, A. S., Jacobsen, G., Drysdale, R. & Erskine, W. 2014: Dating recent floodplain sediments in the Hawkesbury-Nepean River system, eastern Australia using single-grain quartz OSL. *Boreas 43*, 1–21.
Smedley, R. K., Duller, G. A. T., Rufer, D. & Utley, J. E. P. 2020: Empirical assessment of beta dose heterogeneity in sediments: implications for luminescence dating. *Quaternary Geochronology 56*, 101052, https://doi.org/10.1016/j.quageo.2020.101052.
Stokes, S., Bray, H. E. & Blum, M. D. 2001: Optical resetting in large drainage basins: tests of zeroing assumptions using single-aliquot procedures. *Quaternary Science Reviews 20*, 879–885.
Summa-Nelson, M. C. & Rittenour, T. M. 2012: Application of OSL dating to middle to late Holocene arroyo sediments in Kanab Creek, southern Utah, USA. *Quaternary Geochronology 10*, 167–174.
Thomsen, K. J., Murray, A. S. & Bøtter-Jensen, L. 2005: Sources of variability in OSL dose measurements using single grains of quartz. *Radiation Measurements 39*, 47–61.
Thomsen, K. J., Murray, A. S., Bøtter-Jensen, L. & Kinahan, J. 2007: Determination of burial dose in incompletely bleached fluvial samples using single grains of quartz. *Radiation Measurements 42*, 370–379.
Thrasher, I. M., Mauz, B., Chiverrell, R. C. & Lang, A. 2009: Luminescence dating of glaciofluvial deposits: a review. *Earth-Science Reviews 97*, 133–146.
Tucker, G. E. 2004: Effect of limited storm duration on landscape evolution, drainage basin geometry, and hydrograph shapes. *Journal of Geophysical Research, Earth Surface 109*, F3, https://doi.org/10.1029/2003JF000032.
Tucker, G. E., Mccoy, S. W., Whittaker, A. C., Roberts, G. P., Lancaster, S. T. & Phillips, R. 2011: Geomorphic significance of postglacial bedrock scarps on normal – fault footwalls. *Journal of Geophysical Research 116*, F01022, https://doi.org/10.1029/2010JF001861.
Wallinga, J. 2002: Optically stimulated luminescence dating of fluvial deposits: a review. *Boreas 31*, 303–322.
Williams, M. A. J., Pal, J. N., Jaiswal, M. & Singhvi, A. K. 2006: River response to Quaternary climatic fluctuations: evidence from the Son and Belan valleys, north-central India. *Quaternary Science Reviews 25* (19-20), 2619–2631.
Wintle, A. G. & Murray, A. S. 2006: A review of quartz optically stimulated luminescence characteristics and their relevance in single-aliquot regeneration dating protocols. *Radiation Measurements 41*, 369–391.

Supporting Information

Additional Supporting Information to this article is available at http://www.boreas.dk.

Data S1. Extended description of field site and modern floodplain depositional environments.

Fig. S1. Simplified geological map of study area (Braden & Ausbrooks 2003). The field location in the study is indicated by the red circle and the Boxley, Ponca and Pruitt discharge gauges are indicated with black circles. The Mississippian–Pennsylvanian sedimentary sequences that sit high in the landscape contribute a significant amount of quartz sediment to the river. The river is currently incising through Mississippi to Ordovician sedimentary sequences that are primarily made up of limestones and dolostones, but with some prominent, massively bedded sandstone units. Ordovician sandstones contribute some quartz sediment material to the river (Keen-Zebert *et al*. 2017).

Fig. S2. A. Google Earth image from 14th April 2019 showing the mid-bar and bar tail locations inundated with water. B. Discharge from Pruitt gauging station 1st March–16th April 2019. Samples were

collected on 19th March 2019 when discharge was ~300 $ft^3\ s^{-1}$ at Pruitt. The peak discharge one month later (14th April) was 1350 $ft^3\ s^{-1}$, typical high-flow level at this time of the year.

Fig. S3. Floodplain top location. Sample BR005 was collected from the hole indicated with the soil knife handle. Note large mature trees on the floodplain surface.

Fig. S4. A. 10-year flood discharge for the Boxley (07055646), Ponca (07055660), Pruitt (07055680) and St. Joe (07056000) USGS river discharge stations vs. drainage area. Locations of discharge stations indicated on Fig. S1. Note, the Pruitt gauge is represented by the grey circle on this graph and was not used in fitting the line; there was not enough data to derive flood discharges for this station. B. Peak discharge from 2008 to 2023 for the Boxley (07055646) and Ponca (07055660) USGS river discharge stations. We estimate that a 20-year flood occurred in 2010.

Table S1. SAR measurement protocol for modern floodplain Buffalo River samples.

Table S2. Calculated recurrence intervals, flood magnitudes and the grain sizes potentially mobilized at the Blue Hole study site. These calculations suggest that the 64–180 mm cobbles on the sampled bar head are potentially mobilized by floods ranging in size from less than 5-year flood to greater than 1000-year flood. Based on our field observations, we believe that the 180-mm cobbles are in fact moved by flood events smaller than the 1000-year flood. Due to the difficulty of calculating the initiation of sediment transport, we suggest that these calculations be used as approximate guidelines.